From nanowires to super heat conductors

Lin Yang,[1] Ravi Prasher,[1] and Deyu Li[2,*]

[1]*Energy Technology Area, Lawrence Berkeley National Laboratory, Berkeley, CA, 94720 USA*
[2]*Department of Mechanical Engineering, Vanderbilt University, Nashville, TN, 37235 USA*

[*]*E-mail: deyu.li@vanderbilt.edu*

Abstract

Thermal transport through various nanowires has attracted extensive attention in the past two decades. Nanowires provide an excellent platform to dissect phonon transport physics because one can change the wire size to impose systematically varying boundary conditions that can help to distinguish the contributions of various scattering mechanisms. Moreover, novel confinement phenomena beyond the classical size effect promise opportunities to achieve highly desirable properties. Based on a summary of research progresses in nanowire thermal properties, we discuss more intriguing observations due to the classical size effect, coupling between mechanical and thermal properties, and divergent thermal conductivity as a result of conversion from three-dimensional to one-dimensional phonon transport, showcasing the superdiffusive thermal transport phenomenon as predicted by Fermi, Pasta, Ulam, and Tsingou (FPUT) in 1955. We hope that these discussions could provide new perspective on further exploring thermal transport in nanowires, which may eventually lead to breakthroughs such as achieving thermal conductivity values higher than that of any known materials.

Introduction

In 1951, Sir R. E. Peierls wrote: "It seems there is no problem in modern physics for which there are on record as many false starts, and as many theories which overlook some essential feature, as in the problem of the thermal conductivity of nonconducting crystals."[1] The statement indeed well reflected the complexity related to lattice thermal conductivity (κ), which originates from the broad-band phonon spectrum, temperature-dependent phonon spectral distribution, and the complex phonon scattering processes involving phonon-phonon, phonon-defect, phonon-electron, and phonon-boundary interactions. The intensive studies of the thermal conductivity of various nanowires in the past two decades not only reveal interesting properties of these emerging materials, but also provide great opportunities to clarify the puzzle related to lattice thermal conductivity.

Successful growth of nanowires provides a rich class of nanomaterials that could provide highly desirable properties to benefit a wide variety of applications including energy technology[2–7] and biomedical applications.[8–10] Back in 1993, two seminal papers by L. D. Hicks and M. S. Dresselhaus pointed out that the variation of the density-of-states induced by quantum mechanics in nanowires could provide a new way of designing thermoelectric materials.[11,12] This has triggered a vast amount of research efforts on predicting nanowire based thermoelectric materials.[13–15] Later, it was realized that nanowires' capability of conducting heat could play an important role in other applications.[16] As such, thermal conductivity measurements have been conducted on various nanowires composed of single element semiconductors (such as Si,[17] Ge,[18] and Bi,[19] etc.), and compound semiconductors (such as ZnO,[20] GaN,[21] Bi_2Te_3,[22] GaAs,[23] and GaP,[24] etc.). Investigating thermal transport through various nanostructures helps to unravel phonon transport physics at nanoscale, which facilitates the development of effective heat dissipation strategies for microelectronics.

In terms of the significance of nanowires on the fundamental understanding of thermal conductivity, nanowires provide an important platform to distinguish the relative contributions of various factors. This is because through effectively tuning the strength of boundary scattering as the nanowire diameter is systematically varied, the relative importance of various scattering mechanisms changes. In this sense, altering nanowire size provides a powerful approach to vary the boundary conditions of the black box of phonon transport, and through examining the resulting

thermal conductivity change, invaluable information on the contributions of different scattering mechanisms can be extracted.

The most widely encountered size effects in nanowires is the boundary scattering of charge and energy carriers, widely known as the classical size effect. For simple straight wires of circular cross-sections, the classical size effect can usually be described by a scattering rate proportional to the ratio of carrier velocity and the wire diameter.[17,25] However, the situation can be much more complex for wires that are not straight and of uniform cross-sections,[26–32] which leads to more interesting observations and new strategies to tune the thermal properties of nanowires. Moreover, phonon scattering at the nanowire surface highly depends on the surface morphology and novel phenomena have been reported for wires with very rough surface.[33,34]

Beyond the classical size effect, phonon characteristics are closely related to mechanical properties and for nanowires, it has been shown that either acoustic softening[35–37] or elastic stiffening[38–43] can occur, which could drastically alter the phonon spectrum and lattice thermal conductivity. Yet, complexity introduced through coupled elastic and thermal property changes are only experimentally demonstrated recently,[36,37] which also opens new routes to tune the wire thermal conductivity. In addition, for ultra-thin wires, strong confinement could induce dimensional crossover with one-dimensional (1D) phonons dominating the lattice thermal transport.[44] In this case, abnormal phenomena including phonon hydrodynamic and superdiffusive transport could occur, which has the potential of creating a class of FPUT-type of super heat conductors with thermal conductivity values higher than that of any known materials.

This perspective will review relevant literatures on thermal transport in nanowires, discuss remaining issues in current understanding, and provide an outlook to future research opportunities.

The classical size effect

The classical size effects for free electrons

Compared to semiconductor nanowires, thermal properties of metal nanowires attracted relatively less attention. This is because thermal transport in metals is normally dominated by electrons and the thermal conductivity of metal nanowires can be readily estimated using the Wiedemann-Franz law based on the wire electrical conductivity that is relatively easy to measure. However, the

classical size effect was first studied for metals at low temperatures[45,46] and recently, it has been shown that the classical size effect in metal nanowires could be more complex than expected.[47,48]

The classical size effect emerges when the carrier mean free path (mfp), the average distance charge or energy carriers propagate between two consecutive scattering events, is larger than the characteristic size of materials. The effect was first realized for free electrons at ultra-low temperatures (~3.8 K, liquid helium temperature), and pioneering studies were conducted by Fuchs and Sondheimer, who introduced the framework of modifying the electrical conductivity of corresponding bulk materials with the Fuchs-Sondheimer (F-S) reduction function.[46,49] The reduction function is derived based on the restriction of electron mfp by surface scattering and initially, the effect is only important at ultra-low temperatures where the electron mfp is very long (~10^{-2} cm) and comparable to rather large sample size. Later the model was directly adopted for transport in metal thin films and nanowires at elevated temperatures because it was believed that the underlying physical mechanisms remained the same.[50–52] An alternative approach is to add a surface resistivity term to the bulk resistivity of metals that can be well described by the Bloch-Grüneisen (B-G) model, which accounts for the effects of electron-phonon and defect scattering on the bulk resistivity of metals.[53]

Given the extensive usage of metal thin films and nanowires in modern technologies, the importance of the classical size effect on the film/wire electrical conductivity/resistivity has been widely recognized. In fact, in 2004, the International Technology Roadmap for Semiconductors abandoned the practice of listing a single bulk value for copper and implemented size-dependent values for the resistivity of copper conductors.[54]

The reduction function is constructed based on ray tracing and observe whether the emitted electrons collide with the film or wire boundaries before they experience electron-phonon scattering. Integrating all emitted electrons from a given cross-section, one can derive the following expression for a metal wire.[55]

$$F(w,h,l_j) = 1 - \sigma\langle w,h,l_j\rangle - \sigma\langle h,w,l_j\rangle, \tag{1}$$

$$\sigma\left\langle w,h,l_j\right\rangle = \left(\frac{6}{4\pi\times wh}\right)\times\int_0^w dx\int_0^h dy\int_{-\arctan\left(\frac{y}{w-x}\right)}^{\arctan\left(\frac{h-y}{w-x}\right)} d\varphi\int_0^{\pi} sin\theta\cos^2\theta\exp\left(\frac{x-w}{l_j sin\theta cos\varphi}\right)d\theta\,. \tag{2}$$

Here w and h are the width and height of the cross section, respectively, and l_j is the carrier mfp in bulk media. The integration is over all directions of azimuthal angle θ, radial angle φ, and from all locations in the cross-section. The boundary resistivity approach assumes that the boundary scattering rate is proportional to v_F/D, where v_F is the Fermi velocity and D is the diameter of the metal wire. It is worth noting that although originally derived considering electron transport, these approaches have been directly applied to phonon transport.[37,56]

It is important to point out that both the F-S reduction function and the boundary resistivity approach assume that different scattering mechanisms are independent from each other, which is the condition that the Matthiessen's rule is valid. Matthiessen's rule simply assumes that the scattering rates calculated separately for each scattering mechanism can be summed as the total scattering rate for charge or energy carriers. However, if implicit interdependence between different scattering mechanisms exists, neither the F-S reduction function nor the boundary resistivity could provide a satisfactory prediction of the nanowire electrical resistance. One such case has been disclosed very recently with the study of electrical resistivity of silver and copper nanowires.[48]

In the past two decades, a number of studies have attempted to model the electrical resistivity of metal thin films[57–59] and nanowires[60–62] over a wide temperature range. It was found that B-G like models could in general satisfactorily fit the experimental data, with a much enhanced residue resistance at low temperatures.[63,64] It was believed that because boundary scattering simply introduces a constant electron scattering rate that is proportional to v_F/D, the boundary resistivity remained approximately constant in the entire temperature range, which could be combined with the residue resistivity due to defect scattering.[64,65] However, a caveat in these studies is that the Debye temperature obtained from the best fitting result is always remarkably lower than the well-accepted value for the given metal.[61,62,64–66] Some attempts have been made to explain this discrepancy. For example, it was hypothesized that softening occurs for surface phonon modes, leading to reduced Debye temperatures.[62,67–69] This is, however, inconsistent with the mechanical property measurement of silver nanowires documenting significant elastic stiffening with enhanced Young's moduli.[70–72]

Very recently, it was suggested that the much reduced Debye temperature from the B-G model fitting is due to the coupling between boundary scattering and electron-phonon scattering.[48] Shown

as in Fig. 1a-b, at elevated temperatures, electron-phonon scattering occurs mainly through large angle scattering, which alters both the energy and momentum of electrons, while as temperature decreases, small angle scattering, which largely conserves the momentum of electrons, becomes important. This renders different boundary scattering rates for electrons emitted at different included angles with the wire axis at lower temperatures.[48] Electrons emitted with a small angle from the wire axis have to experience multiple times of scattering with phonons to achieve a significant change in their traveling directions before collision with the wire surface. In comparison, electrons emitted with a large angle from the wire axis tend to collide with the wire surface directly. Importantly, the varying contributions of large and small angle scattering leads to a temperature dependent coupling between boundary and electron-phonon scattering; and therefore, modeling based on the Matthiessen's rule without explicitly considering the interdependence between boundary and electron-phonon scattering yields a Debye temperature much lower than the corresponding value extracted based on the material heat capacity.[48] Based on this understanding, a model taking into account the different contributions of electrons emitted at large and small angles from the wire axis can fit the experimental data of copper and silver wires very well while adopting realistic Debye temperatures of these materials (Fig. 1 c-d).[48]

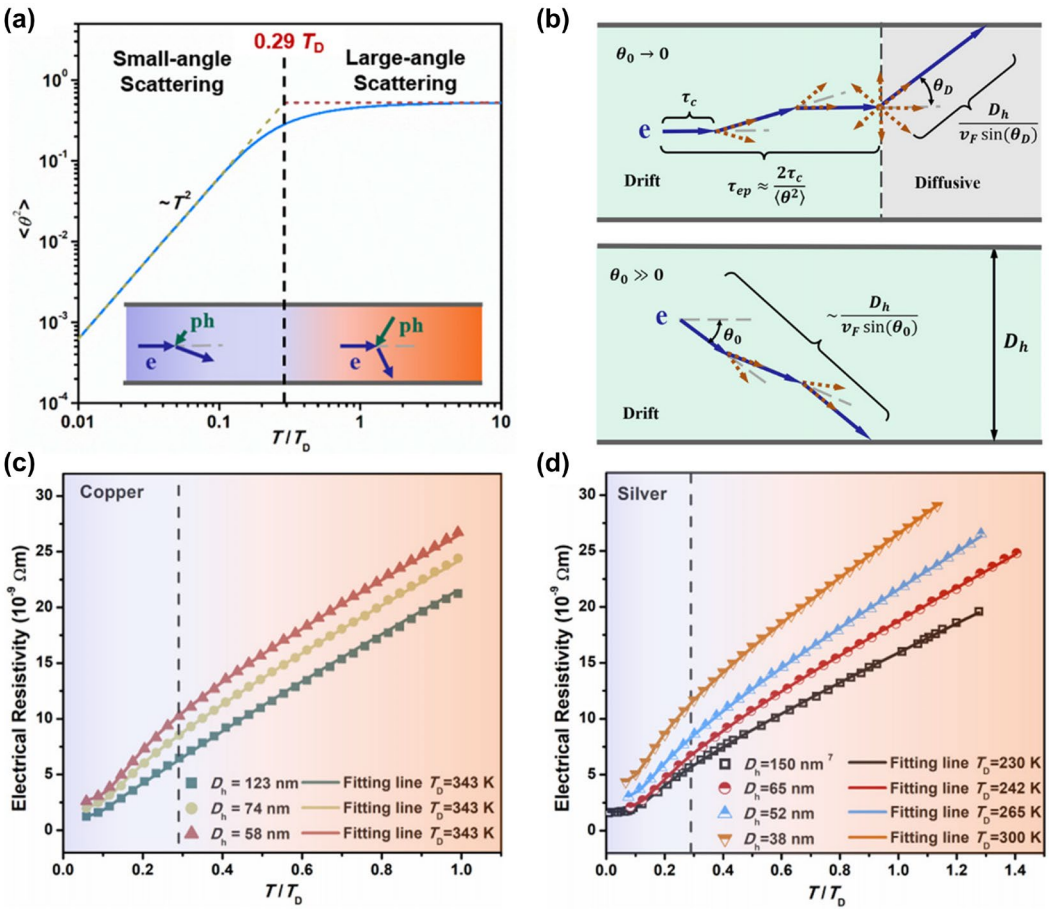

Figure 1. (a) Electron scattering angle (θ^2) as a function of the ratio of temperature *(T)* over Debye temperature (T_D). (b) Schematic illustrations of the transport process in the metal nanowire for electrons with small emission angles and relatively large emission angles. Electrical resistivity of (c) copper and (d) silver nanowires with different diameters. Reproduced from Y. Tao, Y. Zhao, M. Akter, T.T. Xu, Y. Chen, and D. Li, Appl. Phys. Lett. 118, 153105 (2021), with the permission of AIP Publishing.

This recent development of the classical size effect for free electrons in metal nanowires indicates that while the physical picture of boundary scattering is straightforward, complications can occur when boundary scattering couples with other scattering mechanisms, in which case the Matthiessen's rule cannot be applied directly without explicitly considering the interdependence between different scattering rates. In fact, more abnormal phenomena can occur when different scattering mechanisms cannot be treated as independent from each other, and caution has to be used in explaining these "novel" observations. The reduced Debye temperature from fitting the electrical resistivity of silver nanowires using the B-G like model provides a good example for this.

The classical size effect for phonons

Compared to the case for electrons, the classical size effect for phonons could be more complex and attracted more attention in the past two decades.[73,74] One important conclusion drawn from intensive studies is that phonon mfp could be much longer than that evaluated using a gray model.[75–77] In fact, even along the *c*-axis of graphite with weak van der Waals interlayer interactions, the phonon mfp has been shown to be well over 100 nm, much longer that the traditionally believed value of just a few nanometers.[78–81] Coupled with the broad band nature of phonons, the widely existing classical size effect as a result of the long phonon mfp leads to a plethora of interesting observations.[78,82–85]

The first experimental study of nanowire thermal conductivity was done with individual silicon nanowires of different sizes,[17] with the then newly developed micro-thermal bridge approach.[86,87] For the microthermal bridge measurement scheme, a microdevice consists of two suspended SiN_x membranes with integrated Pt heaters/resistance-thermometers and extra electrodes is used, and a nanowire sample is placed between the two membranes.[86,88,89] During the measurement, one Pt resistor serves as a heater to increase the temperature of the suspended membrane, and both Pt resistors serve as resistance thermometers to measure the temperatures of both the heating and sensing membranes. The thermal conductance of the nanowire can be extracted based on the total power dissipation and the temperature rise of the membranes. More details of this measurement technique can be found in the literature.[86,90] The measured data demonstrate a strong diameter dependence, indicating the classical size effect.[17] However, challenges have been encountered in recapturing the experimental data through modeling. Back in the 1950s and 1960s, Callaway and Holland separately fit the thermal conductivity of Si and Ge almost perfectly over a wide temperature range,[91–93] and because of the impressive match between the experimental data and the modeling results, their expressions of the phonon-phonon scattering rate were widely adopted. However, initial modeling efforts through directly combining the expressions for scattering mechanisms in bulk Si from either Callaway or Holland with the boundary scattering rate for phonons, v/D, where v is the speed of sound, failed to reproduce the experimental trend.[25] Luckily, an expression for the phonon-phonon scattering has been proposed in another study of the thermal conductivity of bulk Ge with different isotope compositions, another approach to vary the "boundary conditions".[94] Shown as in Fig. 2a, adopting the then newly proposed term for phonon-phonon scattering together with the calculated phonon dispersion for Si nanowires,

theoretical model was able to recapture the measured thermal conductivity of three large diameter Si nanowires well.[25,95]

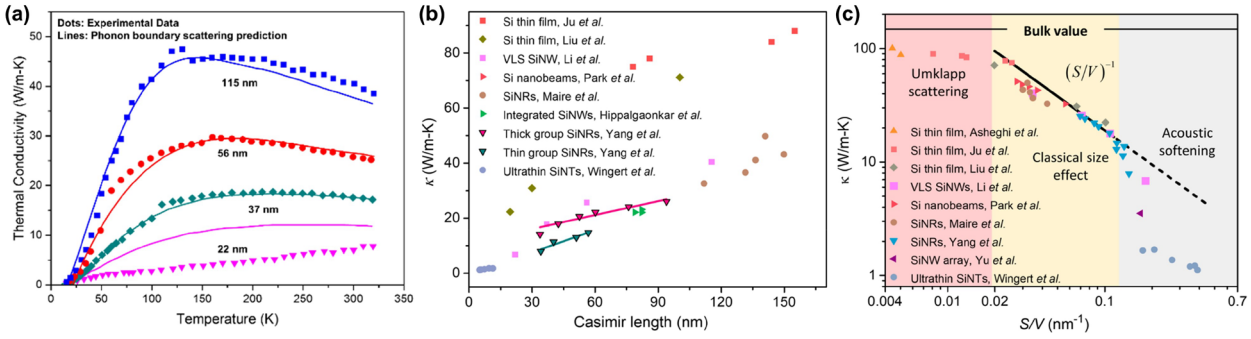

Figure 2. (a) Measured thermal conductivity of Si nanowires with different diameters,[17] and the modeled results based on phonon boundary scattering are also plotted for comparison.[25] Room temperature (300 K) thermal conductivities of various silicon nanostructures versus their (b) Casimir lengths and (c) surface-area-to-volume ratios (*S/V*). (b-c) Reproduced with permission from Chem. Rev. 119, 9260 (2019). Copyright 2019 American Chemical Society.

One issue in describing the classical size effect for phonons is the parameter to characterize the size of the nanowires if their cross-sections are not circular. Historically, the Casimir length, L_c, which is essentially the equivalent diameter of a circle with the same area as the irregular wire cross-section, was adopted for this purpose. For example, for circular nanowires, L_c is wire diameter D, and for nanowires with rectangular cross-sections, $L_c = 2\sqrt{wt}/\sqrt{\pi}$, where w and t are width and thickness of the cross-section, respectively. For thin films, L_c is the limiting dimension, *i.e.*, film thickness. However, when the measured thermal conductivity of Si rectangular nanoribbons was plotted against L_c (Fig. 2b), it was found that very different thermal conductivities could exist for ribbons with different aspect ratios but of the same Casimir length.[37] This indicates that the Casimir length cannot properly characterize the boundary scattering strength and is not a good descriptor to quantitatively determine the classical size effect. Instead, Fig. 2c shows that, different from the randomly scattered data points for κ plotted against L_c, the measured κ *versus* the surface-area-to-volume ratio (*s/v*) of various Si nanostructures collapsed to form an inversely linear relationship, which suggests that *s/v* is a better descriptor for the phonon-boundary interactions.[37] Physically this is reasonable because *s/v* represents the relative importance of surface while the Casimir length only emphasizes the equivalence of the cross-sectional area. It is worth noting that recently, the hydraulic diameter, four times the reciprocal of the *s/v*, which is

more consistent with the size effect, has been adopted to characterize the size of non-circular nanowires, including quasi-1D van der Waals crystal nanowires obtained from liquid exfoliation method,[96–98] Ag nanowires with pentagonal cross-section,[52] and porous Si nanowires.[99]

In addition to silicon nanowires, the thermal conductivities of various nanowires of other materials have been measured and in general, significant reduction from the bulk value as a result of the classical size effect has been observed.[20,21,100–103] Again, for studies with varying diameters, the imposed boundary scattering at different levels served as variable "boundary conditions" helping to elucidate the phonon transport mechanisms in these nanowires.

In addition to a simple straight configuration, nanowires of more complex morphologies, such as kinked[26,27] and fish-bone wires,[29,30,104] have recently been fabricated and measured. Building on the existing knowledge on the classical size effect, the newly accumulated understanding helps to establish the design rules to enable a tight control of phonon transport and engineer functional thermal materials with new degrees of freedom. For example, a numerical study based on non-equilibrium molecular dynamics (NEMD) simulations predicted that a single kink in a thin silicon nanowire could reduce the thermal conductivity by 20%, which was explained based on the required phonon mode interchange and a pinching effect at the kink regime.[105] Experimental demonstration of the kink effect on thermal transport only became available recently and disclose more insights.[26,27]

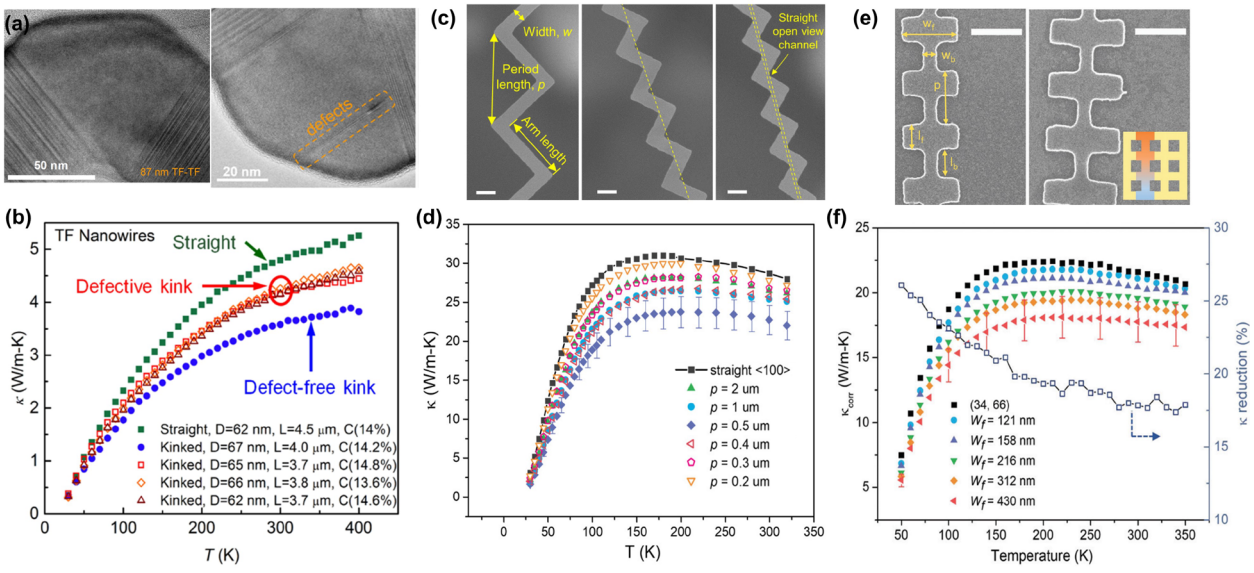

Figure 3. (a) TEM images of kinked boron carbide nanowires with defect-free and defective kink. (b) Measured thermal conductivity of boron carbide nanowires that are straight, with defect-free

kinks, and with defective kinks, respectively. (a-b) Reproduced with permission from Nano Lett. 17, 3550 (2017). Copyright 2017 American Chemical Society. (c) SEM images of kinked Si nanoribbons with the same cross section (33 nm thick, 141 nm wide) and same crystalline direction (⟨100⟩) but different period lengths, p. All the scale bars are 200 nm. (d) Measured thermal conductivity of the six kinked Si nanoribbons of 34 nm thick- ness, 141 nm width, and all patterned along the ⟨100⟩ crystalline direction but with different kink period lengths, where the corresponding straight Si nanoribbon is also plotted for comparison. (c-d) Reproduced from L. Yang, Q. Zhang, Z. Wei, Z. Cui, Y. Zhao, T.T. Xu, J. Yang, and D. Li, J. Appl. Phys. 126, 2 (2019), with the permission of AIP Publishing. (e) SEM images of Si fishbone nanoribbons, where all dimensions are kept the same but only the fin width, w_f, is changed across different samples. The inset image shows that fishbone nanoribbons could be regarded as building blocks for nanomeshes with aligned hole arrangement. (f) Temperature dependent corrected thermal conductivity for five different Si fishbone nanoribbons, where the measured κ of the straight ribbon is also plotted for comparison. The calculated thermal conductivity reduction for the fishbone nanoribbon with the fin width of 430 nm is plotted as a function of temperature (right axis). (e-f) Reproduced with permission from Nanoscale 11, 8196 (2019). Copyright 2019 Royal Society of Chemistry.

Through systematic measurements of straight and kinked boron carbide nanowires, Zhang et al. found that a single kink could lead to 36% thermal conductivity reduction for a nanowire of 87 nm diameter and 4.3 μm long (Fig. 3a,b).[26] The remarkable kink thermal resistance is attributed to backscattering of highly focused phonons at the kink. The argument is strongly supported by the finding that defects in the kink, instead of posing additional resistance, could actually facilitate phonon transmission through the kink via scattering phonons into the opposite arm. To further understand the kink effects on phonon transport, as shown in Fig. 3c, Si nanoribbons with multiple kinks and systematically varied kink period length were measured.[27] Owing to the much weaker elastic anisotropy compared with boron carbide, phonons are not strongly focused in Si and the backscattering effect is not as significant. As such, a single kink in the Si nanoribbons poses much lower resistance, where a maximum κ reduction of 21% is observed for a nanoribbon with multiple kinks at room temperature (Fig. 3d).[27] Importantly, it was found that as the period length drops to a level at which a straight heat transfer channel opens between the heat source and heat sink, κ exhibits a sharp increase trend.[27] These results provide important guidelines on modulating heat transfer in nanostructures using kinks, which could be adopted to tune the thermal properties of nanostructures for different applications.

It is important to note that the significant difference of kink effect on thermal transport between boron carbide and silicon nanowires points to coupling between the phonon backscattering effect and phonon focusing. In boron carbides, phonons are focused to travel along the wire axis direction

and backscattering at the kink boundary poses significant resistance.[26] On the other hand, for silicon, phonon focusing effect is weak and phonons travel along all directions. In this case, phonon reflection at the kink boundary is more isotropic and the kink presents much weaker resistance as compared with that for boron carbide.[27]

Apart from kinked nanowires, another type of nanowires that have drawn attention is the fishbone wires prepared through top-down fabrication with periodical fins attached to a backbone nanoribbon.[29,30,104] The artificially engineered periodic nanostructures with periodicity on the order of phonon wavelength are sometimes also referred to as phononic crystals. The wave interference developed within these periodic structures could give rise to exotic effects, such as Brillouin zone folding and bandgap formation, which are not observed in conventional bulk crystals. Although this concept has been applied to explain the measured ultra-low room temperature κ of Si nanomeshes,[106,107] another type of phononic crystal, it should be noted that phonon coherence requires very strict conditions to maintain their phase and frequency, which renders the wave effects only important at ultra-low temperatures in the milli-Kelvin range. Instead of modification of the phonon dispersion as a result of phonon wave interference, it has been suggested that diffusive phonon scattering within the complex nanostructures is responsible for the measured low κ at room temperature.[108,109]

To experimentally distinguish the effects of phonon interference and boundary scattering, fishbone nanoribbons with fixed periodicity but different fin width were measured, as shown in Fig. 3e.[29] A monotonically decreasing trend of κ is observed as the fin width increases, reaching a maximum κ reduction of 18% at 300 K. As both the period length and the limiting dimension are kept the same, the reduced thermal conductivity should not be the result of either phonon coherence or stronger phonon boundary scattering. Instead, the κ reduction is attributed to the ballistic thermal constriction resistance, *i.e.*, Sharvin resistance, induced by the cross-section constriction between the fin and backbone sections.[29] It is worth noting that so far, at elevated temperatures, phonon coherence effects have only been observed in superlattices with nearly perfect interfaces between the alternating layers,[110,111] while no unambiguous conclusion has been reached for other types of phononic crystals. This is in part due to the short wavelength of thermal phonons at elevated temperatures, and also the difficulty to directly measure the phonon coherent length. Recently, two-photon interference methods such as coherent population trapping and electromagetically induced transparency has been proposed to measure the phonon coherence length,[112] which could

potentially unravel the rich physics. Hopefully, improved understanding of the phonon coherence and more advanced techniques/instrumentation would allow for phononic engineering at elevated temperatures, which will lead to new frontiers of discovery.

Apart from phonon coherence, quantum effects of phonon transport could become important at cryogenic temperatures. As experimentally demonstrated by Schwab *et al.*,[113] at temperatures below 1 K, as the phonon wavelength becomes comparable to or even larger than the size of a constriction in a SiN_x phonon waveguide, only four lowest lying phonon modes, namely one dilatational, one torsional, and two flexural modes, are allowed to propagate within the structure, and the measured thermal conductance represents the limiting value of universal quantum thermal conductance. This research opened the door for exploring phonon transport in the quantum confinement regime. However, due to the ultra-low temperatures involved, and challenges associated with ultra-sensitive thermal conductance measurements, there are only a few following-up work on this topic,[114,115] and probing and engineering quantum effects of thermal transport remains a difficult subject.

Coupling between mechanical and thermal properties

Since phonons are the quanta of lattice vibration waves, phonon properties are highly correlated with the mechanical properties of the lattice. In fact, almost all formulas predicting the lattice thermal conductivity include some information related to the mechanical properties of the materials. For example, the kinetic theory predicts a most simplified formula, $\kappa = 1/3\, Cvl$, where C is the heat capacity per unit volume, v is the speed of sound and l is the phonon mfp. In this formula, the speed of sound is directly related to the mechanical property, Young's modulus (E) through $v = \sqrt{E/\rho}$, where ρ is the density of the material. Moreover, the speed of sound also plays an important role in phonon dispersion, which is important in determining the heat capacity. Another widely known formula proposed by Slack for bulk nonmetallic crystals at high temperatures (higher than the Debye temperature, θ) is $\kappa = A\frac{\bar{M}\delta\theta^3}{\gamma^2 T N^{2/3}}$, where A is a proportional constant, N is the number of atoms in the unit cell, $\bar{M}$ is the mean atomic mass while δ^3 is the average volume of each atom, and γ is the Grüneisen parameter.[116] In this formula, both the Grüneisen parameter and the Debye temperature are strongly correlated with the mechanical properties of the materials. In fact, it is widely believed that materials with stiff bonds usually have a high κ.

While the coupling between mechanical properties and lattice thermal conductivity has been known, the connection between these two properties for nanowires was made only recently,[36,37] after separate studies of each property for more than a decade.[17,35] Depending on the reconstruction of the surface atoms, the Young's modulus of nanowires can be either reduced or enhanced, which corresponds to phonon softening (acoustic softening) and hardening (elastic stiffening). While the understanding of the effects of elastic property modulation on lattice thermal conductivity of nanowires is not complete yet, the mechanical property modulation offers a fundamentally distinct avenue to tune and engineer thermal transport in nanowires beyond the classical size effect.

Acoustic softening effects

The effect of acoustic softening on nanowire thermal conductivity, while only realized in 2015, actually manifested its significance in the first set of thermal conductivity data for silicon nanowires.[17,36] As mentioned previously, through adopting the full dispersion relation, good agreement was achieved between the model prediction and experimental data for the three larger diameter silicon nanowires with diameters > 37 nm.[25,95] However, even many attempts considering various factors have been made, no satisfactory fitting could be achieved for the measured κ of the 22 nm diameter silicon nanowire.[25,95,117–120] Two main discrepancies are that (1) the experimental data are lower than the theoretical predictions, and (2) the temperature dependence cannot be well explained. While there have been questions about possible experimental errors in the experimental data, similar behavior has also been observed in thin Ge nanowires, where the measured κ deviates from the phonon boundary scattering prediction drastically for wires with diameters smaller than 15 nm.[121]

The intriguing behavior of the thermal conductivity of thin Si and Ge NWs has attracted a great deal of attention without convincing physical explanations until 2015, when Wingert et al. reported a systematic study of ultra-thin silicon nanotubes with wall thickness as small as 5 nm.[36] It was found that the silicon nanotubes displayed κ values much lower than the prediction only taking the classical size effect into account; and in fact, the measured κ values are even lower than that of amorphous silicon nanotubes of similar dimensions.[36] As shown in Fig. 4a, a breakthrough in their study is to correlate the obtained κ with the Young's modulus of thin silicon nanowires measured from the elastic tensile tests, which demonstrates a sharp reduction from the corresponding bulk value as the wire diameter became smaller than 30 nm.[35] The elastic property characterization on

the silicon nanotubes was performed, which yielded Young's modulus up to six-fold lower than the bulk value. Since $v \propto \sqrt{E}$, the drastically reduced Young's modulus corresponds to a much lower thermal conductivity according to $\kappa = 1/3\, Cvl$. This study provides the first satisfactory explanation of the lower than expected thermal conductivity of thin Si and Ge nanowires and connects the mechanical and thermal properties of nanowires for the first time.[36]

While Wingert et al.'s study represents a critical advancement, concerns have been raised regarding whether the reduced Young's modulus is due to structural defects introduced in the synthesis process, which could also lead to reduced thermal conductivity through enhanced defect scattering. In addition, the silicon nanotubes in Wingert et al.'s study are of nearly identical dimension, it would be desirable to explore the transition dimension at which the acoustic softening starts to affect thermal transport, which is critical for providing important design rules in engineering the mechanical properties of nanostructures to tune their thermal conductivities. To address these issues, a follow up work on Si nanoribbons (SiNRs) of two different thicknesses (~20 and 30 nm) and different widths, and hence different cross-section aspect ratios were conducted.[37] The SiNRs were prepared using top-down approach through nanofabrication from high-quality single crystalline device silicon layers of silicon-on-insulator wafers. In this way, there should be minimal defects; and if any, their concentrations should be the same for these two groups of SiNRs of different thicknesses.

The elastic properties of individual nanowires can be experimentally measured using a three-point bending test with an atomic force microscope.[122,123] This method has been previously used to measure the Young's modulus of various nanostructures, such as Si nanowires,[37,123] ZnO nanowires,[124] polymer nanofibers,[125] etc. For this measurement, the Young's modulus is extracted from the force–deflection curve recorded during the extension and retraction process in the bending test. Through comparing the measured κ and E, it is found that (1) E of the 30 nm thick ribbons is very close to the bulk value and the measured κ can be well-accounted for by the classical size effect, indicating the low structural defect concentration and high crystal quality of the ribbons; and (2) for ribbons in the 20 nm thick group with hydraulic diameter D_h smaller than 33 nm, e.g. $s/v > 0.12$ nm^{-1}, the measured E is significantly lower than the bulk value, and meanwhile the measured κ deviates from the prediction based on the classical size effect (Fig. 4b).[37] Collectively, these observations point to the effects of acoustic softening on thermal

conductivity, which helps to complete the regime map for κ versus nanostructures' D_h that clearly delineates the two regimes where acoustic softening is important or not.[37]

Theoretically, the Young's modulus of single crystalline materials depends heavily on its interatomic bonding energy and lattice structure. For the surface Si atoms, owing to the lower coordination numbers and electron densities compared to their bulk counterpart, they tend to adopt different bond spacing, leading to an association energy different from those in the core.[36] As such, the reduced Young's modulus of the Si nanostructures could be explained based on an approximate core-shell composite model with the surface shell atoms of a different morphology from the core atoms.[43] In this model, the core has the elastic modulus of the corresponding bulk material, E_0, while the surface shell possesses a surface modulus E_s; and the value E_s/E_0 becomes a critical parameter determining the tendency of the size dependence of a nanowire's Young's modulus. Although elastic property change has been identified to be responsible for the ultra-low κ of thin Si nanostructures, a full scope study of all changes in the heat capacity, phonon group velocity and mfp from the Young's modulus change in thin nanowires should be carried out to dissect how different factors contribute to the κ reduction. Finally, further study is still needed to glean insights into the temperature dependence of the thermal conductivity of thin Si and Ge nanowires.

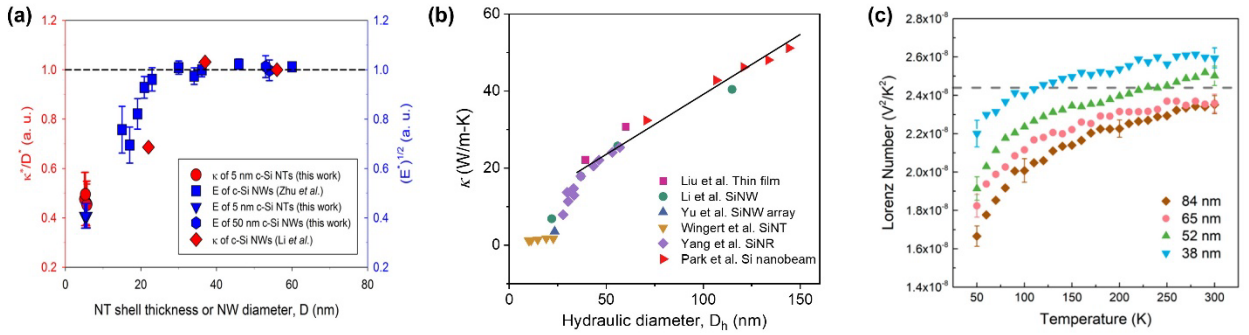

Figure 4. (a) Correlation between thermal conductivity (κ) and elastic modulus (E) in crystalline NTs and NWs. κ, D, and E have been normalized with their respective values for ~60 nm Si NWs and plotted as a function of D, where D is the shell thickness for NTs or the diameter for NWs, whichever applicable. Normalized variables are labeled as κ^*, D^*, and E^*, respectively, and the dashed line represents the maximum of both κ/D and √ E. Reproduced with permission from Nano Lett. 15, 2605 (2015). Copyright 2015 American Chemical Society. (b) Room temperature (300 K) thermal conductivities of various silicon nanostructures[17,36,37,56,106,126] versus their hydraulic diameter, D_h, which is four times the reciprocal of surface-area-to-volume ratio (S/V). This clearly shows two regimes where size effects beyond phonon-boundary scattering are important or not. (c) Derived Lorenz number of four different diameter silver nanowires. The gray dash line labels

the Sommerfeld number. Reproduced with permission from Nano Lett. 20, 7389 (2020). Copyright 2020 American Chemical Society.

Elastic stiffening effects

Contrary to acoustic softening, there have been reports for several types of nanowires, including Ag,[38–40] Pb,[41] GaN,[42] and ZnO[43] wires, whose Young's moduli increase as their diameters decrease, which is known as elastic stiffening and can lead to phonon hardening effect. As mentioned previously, E_s/E_0 represents a critical parameter determining the tendency of the size dependence of the Young's modulus, and the enhanced Young's modulus could be partly attributed to the opposite surface atom bonding condition compared with that of silicon. However, to date, there have been very limited studies on the effects of elastic stiffening on the thermal conductivity of these nanowires. We note that Bui et al. conducted a thermal conductivity measurement on ZnO nanowires with diameter reducing from 209 to 70 nm, which showed a continuously decreasing κ without signs of any Young's modulus change.[20] This could be due to the fact that the smallest pristine nanowire they measured is still 70 nm diameter,[20] while remarkable Young's modulus enhancement for ZnO nanowires only occurs in wires of < 50 nm in diameter according to Chen et al.[43]

Recently, through systematic electrical and thermal transport properties measurements of silver nanowires (AgNWs) with diameters ranging from 38 to 84 nm, Zhao et al. demonstrated that the contributions of phonons become more significant as a result of elastic stiffening.[52] From the temperature dependent Lorenz number, it is shown that the nanowire of 84 nm diameter has a comparable Lorenz number with bulk silver at room temperature, and as temperature decreases, the Lorenz number of the nanowire becomes higher than the bulk value (Fig. 4c). Moreover, as the wire diameter reduces, the Lorenz number becomes higher over the whole temperature range and could even rise beyond the Sommerfeld value.[52] Detailed analysis indicates that the enhanced effective Lorenz number is due to enhanced contribution of lattice thermal conductivity, which could be three times higher than the corresponding bulk value. The enhancement in the lattice thermal conductivity is further attributed to elastic stiffening, which could induce several changes in phonon transport.[52]

First, elastic stiffening corresponds to a higher speed of sound, which is directly proportional to the lattice thermal conductivity (κ_{ph}). In addition, the higher Debye temperature θ shifts the phonon

distribution to lower wave vectors at any given temperature, which should reduce the Umklapp scattering rate. Moreover, the e-ph scattering rate also becomes smaller as it is inversely proportional to θ, which corresponds to a reduced e-ph scattering rate in smaller wires. We note that only thermal and electrical conductivities of the AgNWs were measured in Zhao et al.'s study, while the Young's modulus results are borrowed from a separate work.[38] It would be desirable to conduct coupled electrical/thermal/mechanical property measurements on the same sample to directly correlate these properties. In addition, it would be highly desirable to examine the effect of elastic stiffening on thermal transport in other material systems, such as ZnO and GaN nanowires, whose thermal conductivity is dominated by phonon transport with negligible electronic contributions. These studies could help to elucidate the elastic stiffening effect on phonon transport without the complication from e-ph scattering.

The neglected elastic stiffening/acoustic softening effects in core-shell nanowires

Heterostructure semiconductor nanowires, such as core-shell structures have attracted significant attention because of their remarkable electronic, optical, and thermal properties as well as potential applications as building blocks for nanoelectronics,[127] nanophotonics,[128] photovoltaics,[129] and thermoelectrics.[130] Understanding thermal transport in core-shell nanowires is crucial for their potential applications; however, previous studies have paid little attention to the possible tuning of the elastic properties in the core-shell nanowires.

Early theoretical studies have focused on the coupling of phonons between the core and shell structures, which highly depends on acoustic impedance mismatch between the core and shell.[131] Later, Hu et al.[132] and Chen et al.[133] performed molecular dynamics (MD) simulations on κ of Si-Ge and Ge-Si core-shell nanowires. Their results show that the core-shell structure strongly suppressed κ as compared to uncoated Si or Ge nanowires, which is attributed to the suppression and localization of long-wavelength phonon modes and the high-frequency non-propagating diffusive modes at the Si-Ge interface. On the experimental side, the thermal conductivity of individual Ge core-Si shell nanowires with diameters from 10-20 nm were conducted.[121] The results indicated that while Si could have higher κ, the core-shell structure actually led to a comparable or even lower κ than that of the pure Ge NWs.[121] While this is qualitatively in agreement with the previous MD simulations on thin core-shell nanowires, the potential effect of

elastic property variations due to the significant lattice mismatch between silicon and germanium has been neglected.

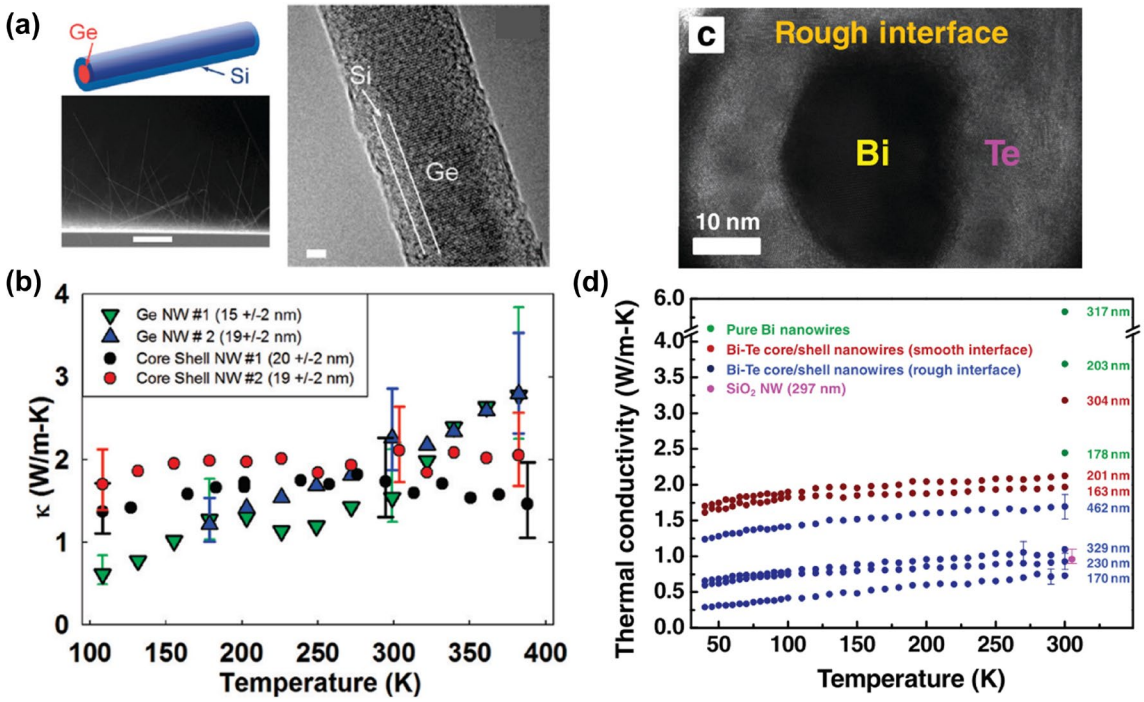

Figure 5. (a) Schematic illustration of a Ge-core Si-shell NW, an SEM image of the side view of Ge−Si core shell NWs grown on a Si substrate (scale bar: 10 μm), and an HRTEM image of a single crystalline Ge−Si core-shell NW (scale bar: 2 nm). (b) Measured thermal conductivity of pristine Ge NWs (green and blue triangles) and Ge−Si core-shell NWs (red and black circles) with diameters ranging from 15−20 nm. (a-b) Reproduced with permission from Nano Lett. 11, 5507 (2011). Copyright 2011 American Chemical Society. (c) High resolution cross-sectional TEM image of a Bi-Te core/shell nanowire. (d) The thermal conductivities of the pure Bi nanowires, the rough interface (RI) Bi-Te core/shell nanowires with d = 170, 230, 329, and 462 nm, and the smooth interface (SI) Bi-Te core/shell nanowires with d = 163, 201, and 304 nm measured in the temperature range of 40 to 300 K. (c-d) Reproduced with permission from Adv. Mater. 23, 3414 (2011). Copyright 2011 WILEY-VCH Verlag GmbH & Co. KGaA, Weinheim.

Another experimental study on individual core-shell nanowires was conducted by Kang et al. on Bi-Te core-shell nanowires.[134] Similarly, a much lower κ was observed as compared to pure Bi nanowires of similar diameter. However, (1) the diameter of the nanowires (d > 170 nm) is much larger than the dominant phonon wavelength and mfps in Bi and Te, so the phonon coherent resonance effect should not be important; and (2) the large diameters result in a relatively low percentage of atoms located proximal to the interface, and thus the κ suppression induced by the interface may not be as pronounced as in the thinner wires. Taken together, phonon transport in

these large nanowires could not be explained by the previous theoretical work on thin core-shell nanowires (~3-12 nm),[131–133] which suggests that factors other than phonon confinement and coherent resonance could play a role. Again, no discussion on the possible change of the elastic properties has been included in this study.

Owing to the lattice constant mismatch between the core and shell materials, it is highly possible that both the core and shell structures in core-shell nanowires are under compression or tensile stress with altered lattice constant.[135,136] If this lattice constant change is beyond the linear regime, the spring constant between neighboring atoms could also depart from the equilibrium value, and together, this could lead to altered mechanical properties, just as the acoustic softening and elastic stiffening effects for single-component nanowires. Given that now it has been confirmed that these effects could have significant impacts on the thermal conductivity of nanowires, it is highly likely the mechanism also plays an important role in thermal transport through core-shell nanowires. Notably, through epitaxially growing WO_3 films on substrates with distinct lattice constants, recent experiments have shown that the lattice thermal conductivity of WO_3 thin films increases upon compression and reduces upon expansion.[135] This provides additional evidence that the elastic property change in core-shell nanowires could be a critical factor whose effect cannot be neglected. Therefore, systematic characterization of core-shell nanowires with simultaneous thermal and mechanical property measurements should be carried out to disclose the contribution of elastic properties in the thermal conductivity of core-shell nanowires, which could lead to an effective approach to tune the thermal properties of nanowires.

Dimensionality transition and FPUT-type of super heat conductors

With two geometric dimensions confined in nanometer scale, nanowires are often referred to as one-dimensional (1D) objects. However, in most cases this designation is purely from a geometric point of view, but not in the physical sense since the wave vectors of electrons and phonons in nanowires are usually not confined to the wire axis direction but distributed along all directions. In this regard, there are two distinct fundamental science questions: (i) at what diameter does a true physical dimensionality transition occur, and (ii) how does such a transition impact carrier transport? These intriguing questions have excited lasting interest with continued efforts of exploring exotic transport phenomena in 1D nanomaterials,[44,137–141] which could offer highly-desirable physical properties that could transform engineering practice in diverse fields.

FPUT problem and its implications to thermal transport in 1D lattices

The question of what happens for phonons in 1D lattices was first numerically studied using the first generation MANIAC electronic computer in 1955, and the unexpected outcome has been known as the classical FPUT paradox.[142] Essentially, the numerical results showed that in 1D lattices with anharmonic interatomic interactions, an excited vibration mode did not dissipate into heat over a long period of time. The FPUT paradox suggests a divergent κ for 1D lattices with the chain length, instead of being a constant value assumed by the Fourier's heat conduction law in the thermodynamic limit.

While the FPUT study is conducted at 0 K initiated with a single vibration mode, later studies of 1D lattices at elevated temperatures also disclose a divergent κ, $\sim L^{\beta}$ ($0 < \beta < 1$), with the system size defined by its linear dimension, L.[143,144] This phenomenon is referred to as superdiffusive thermal transport and has attracted extensive attention because it not only addresses the fundamental issue of how heat is conducted in solids, but also predicted extraordinarily high κ for general 1D lattices with extended but finite length.[44,145,146] In fact, for 1D lattices with sufficient length, the predicted thermal conductivity can often be higher than that of any known materials, *i.e.*, 1D lattices with sufficient length can be regarded as a type of super heat conductors. We note that here super heat conductors do not mean that the thermal resistance drops to zero. In fact, the thermal resistance still increases with the sample length. However, the thermal conductivity of 1D lattices keeps increasing with length and could be well beyond that of any known bulk materials. We call these lattices the FPUT-type of super heat conductors.

Recently, taking advantage of the rapid growth of computational power, a great deal of efforts have been devoted to study anomalous heat conduction in low dimensional nanostructures using numerical simulations.[145,146] These studies provided strong evidence that low dimensional nanostructures are very promising platforms that can be used to examine and verify fundamental thermal transport theories. It is not only of fundamental interest for the development of statistical physics to understand normal and anomalous heat conduction in low dimensional systems, but also of great importance from the application point of view. As the modern nanofabrication technology has enabled one to access and routinely fabricate nanowires with characteristic sizes down to a few nanometers, the anomalous phenomena occurring in 1D systems provide a fundamentally new

avenue to manipulate thermal transport, which could guide the design of high κ materials for efficient heat dissipation of micro/nanoelectronics.

The evolution of theoretical understanding of the FPUT paradox and divergent thermal conductivity of 1D lattices

Early studies on thermal transport through 1D lattices focused on the underlying physics of the recurrence of phonon modes as indicated by the FPUT paradox[147–149], and solitons have been considered to be responsible for the mode recurrence and the divergent thermal conductivity. In fact, significant efforts have been devoted to explore the conditions required to eliminate the solitons to render a normal thermal conductivity[150–152]. In fact, researchers working on thermal transport through 1D lattices were relieved when it was found that a ding-a-ling model[153] could achieve a converged thermal conductivity. However, the debate continues and there have been very recent publications indicating that eventually the excited phonon mode will be dissipated into heat.[154]

The superdiffusive behavior in 1D lattices and the power law divergence of the thermal conductivity gain significant attention in the past three decades. However, many fundamental issues are still in debate. For example, a recent study suggests that instead of solitons, it is low frequency phonons that are responsible for the divergent thermal conductivity in 1D lattices.[154] In addition, significant attention have been paid to the power law dependence for the thermal conductivity of 1D and 2D systems, and explored what type of interatomic potentials give rise to divergent thermal conductivity.[145,155–159] After rather extensive studies in the past two decades, it is becoming a consensus that for 1D lattices with a variety of interatomic potentials, the thermal conductivity diverges with the chain length following a 1/3 power law under the long chain limit; however, there are still some discussions on whether this is a universal law.[160]

Early modeling efforts actually pointed to a power law divergent trend with a different exponent. For example, in 1998, Lepri et al. calculated the thermal conductivity of FPUT chains using a mode coupling theory, which yielded a divergent exponent of 2/5.[155] Later, in 2002, Narayan et al. claimed a divergent exponent of 1/3 for 1D systems based on a renormalization-group calculation of the stochastic hydrodynamic equations. Moreover, they suggested that the 2/5 power law divergence in previous studies was due to an incorrect scaling conversion.[161] One year later, Lepri et al. re-examined the exponent through numerical simulations of 1D lattices of different lengths,

and suggested that instead of 1/3 power law divergence, their results suggested an exponent closer to 2/5, supporting the mode coupling prediction.[157] Later, a kinetic theory calculation[162] and molecular dynamics simulations[158,159] provided additional support to the 2/5 power law divergence. Without experimental validation and a clear understanding of the physical origin, the debate has not been completely resolved yet. However, it is conjectured that the 2/5 exponent is for lattices subjected to purely longitudinal dynamics (i.e., without transverse motion), and it will convert to 1/3 when transverse motions are involved and/or in the long length limit.[145,158,159]

Driven by the desire to unravel the underlying mechanisms for phonon transport in 1D atomic lattices and to achieve highly thermal conductive materials, MD and first-principles simulations have been recently performed to investigate heat conduction in realistic material systems, such as single atomic chains of polymer crystals[163,164] and ultra-thin Si nanowires.[165,166] It has been shown that unlike amorphous bulk polyethylene (PE) with low κ of only ~0.1 W/mK, phonon transport undergoes a dimensional crossover from 3D to 1D with an ultra-high κ of ~130 W/mK in single PE molecular chain.[163,164] This was attributed to the significant attenuation of anharmonic phonon-phonon scattering as transitioning to single chain limit, and the 1D phonon modes propagating along the stiff backbone of covalently bonded polymer chains.[163,164] More recently, through modeling heat transport in ultra-thin Si nanowires of < 3 nm, Zhou et al. found a steep increasing trend in κ as the diameter reduces, which is in stark contrast to the classical size effect predicton.[165] In fact, the modeled κ of a ~0.7 nm Si nanowire is more than one order of magnitude higher than the bulk value.[165] These interesting observations were explained based on the novel phonon hydrodynamic transport phenomena, as induced by the dominant Normal scattering (energy and momentum conserved) process of low frequency acoustic phonons in the ultra-thin nanowires.[165] Collectively, these theoretical efforts provide critical insights into heat conduction in 1D lattices, which will be necessary for identifying and designing high thermal conductivity materials.

Experimental demonstration of superdiffusive transport in 1D systems

Superdiffusive transport in 1D lattices was used to be regarded as of academic interest only, considering the tremendous experimental challenges of preparing single atomic chains of sufficient lengths and measurements of the associated ultra-low thermal conductance. While single atomic chains have been experimentally observed, their lengths are only of about tens of atoms.[138,140] In fact, a recent report showed that thermal transport through these short atomic chains could be

governed by ballistic transport with length-invariant thermal conductance.[138] Efforts on observing superdiffusive transport in low dimensional systems have been made with graphene as the model of 2D systems[167] and carbon nanotube as the model for 1D systems;[168,169] however, critics has been raised about the results.

In 2008, Chang et al. probed the length dependence of the thermal conductivity of carbon nanotubes using a sequential multiprobe scheme through depositing a series of thermal contacts to vary the suspended length of the same sample between the heat source and sink.[168] Figure 6a shows the measurement device with the inset illustrating the nanotube thermally connected to the underlying electrode with the Pt-C composite locally deposited using electron-beam-induced deposition (EBID). Their results indicated length dependent thermal conductivity for carbon nanotubes (CNTs) and boron nitride nanotubes (BNNTs). Attempts have been made to fit the length dependence to the power law of $\kappa \sim L^{\beta}$ (L is the length of the nanotube); however, inconsistent β values were obtained for different samples and a minimum deviation from the power law trend was determined with β ranging from 0.6 to 0.8 for CNTs, and from 0.4 to 0.6 for BNNTs.[168] The maximum sample length for the respective nanotube samples in this study is from ~ 3.8 to ~ 7 μm. At the time of the referred publication, the phonon mfp in CNTs and BNNTs was still thought to be only 1 to 2 μm so the length dependence was believed to be beyond the bulk mfp and violate the Fourier's law. However, later it was shown that phonons with mfp up to ~ 10 μm can still make appreciable contribution to the in-plane thermal conductivity of graphite.[170] Therefore, it is likely that the length dependence Chang et al. demonstrated in 2008 is due to partially ballistic transport of phonons, given that the phonon mfp in CNTs should be comparable to that for phonons in the basal plane of graphite.

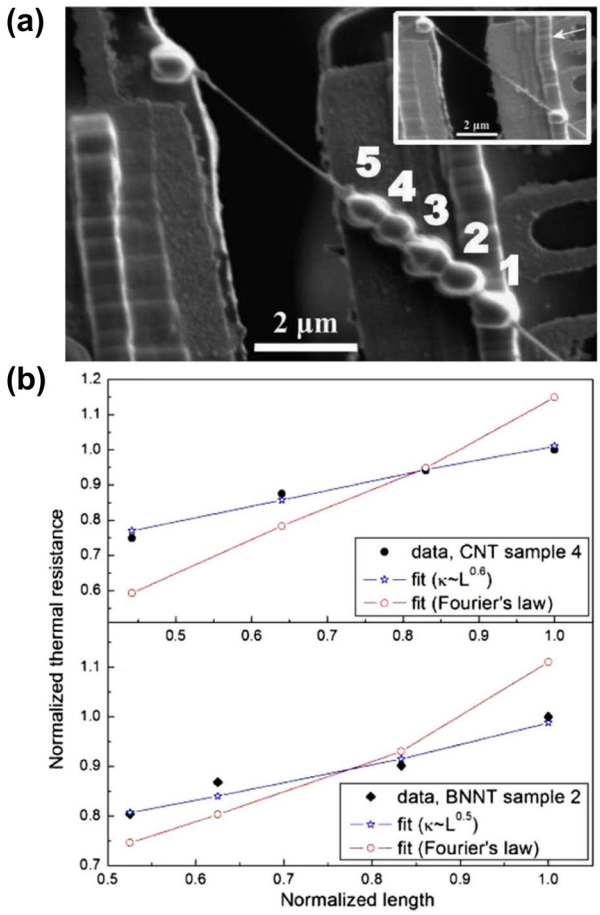

Figure 6. (a) A SEM image of a thermal conductivity measurement device with a boron nitride nanotube (BNNT) after five sequences of $(CH_3)_3(CH_3C_5H_4)Pt$ deposition. The numbers denote the *n*th deposition. The inset shows the SEM image after the first $(CH_3)_3(CH_3C_5H_4)Pt$ deposition. The arrow denotes the pre-formed rib for suspending the BNNT. (b) Upper: Normalized thermal resistance *vs* normalized sample length for CNT sample 4 (solid black circles), best fit assuming power law divergence $\beta = 0.6$ (open blue stars), and best fit assuming Fourier's law (open red circles). Lower: Normalized thermal resistance *vs* normalized sample length for BNNT sample 2 (solid black diamonds), best fit assuming $\beta = 0.4$ (open blue stars), and best fit assuming Fourier's law (open red circles). Reproduced with permission from Phys. Rev. Lett. 101, 1 (2008). Copyright 2008 American Physical Society.

More recently, in 2017, Lee et al. reported observation of divergent thermal conductivity for SWCNTs up to millimeter length with κ values beyond 10,000 W/m-K.[169] However, when fitting with the power law length dependence, again different β values were obtained for different tube samples without a physical ground.[169] More importantly, for several samples, the thermal conductivity first demonstrated a convergence trend when the tube length reached ~ 10 µm before a sudden jump in values when the tube length increased to 100-1000 µm.[169] The interesting results

attracted immediate attention with doubts. While the data certainly call for further study, the journal published a comment suggesting that the data are questionable because the study did not consider (1) the effects of outgoing heat conduction on the temperature profile of the heaters, and (2) the radiation heat loss from the sample surface, which could lead to a higher normal thermal conductivity.[171] Following up discussions have also been posted on ArXiv.[172,173]

We are aware that because of this series of discussions, a misconception that radiation heat loss from the sample surface would lead to a higher nominal thermal conductivity for nanowires for the thermal bridge method is spreading in the community, which is not necessarily true. Whether radiation heat loss would lead to significant deviation of the measured thermal conductivity from the true value depends on the ratio of radiation heat loss to heat conduction through the nanowire. In addition, whether radiation from sample surface leads to a higher or lower measured thermal conductivity than the true value also depends on the thermal resistance network and how the temperature at each node and the heat current are determined in the data reduction process.

In addition to CNTs, the thermal conductivity of 2D graphene of various lengths has also been recently studied, which suggests a logarithmic length dependence, consistent with the predicted superdiffusive phonon transport in 2D lattices.[167] However, the maximum sample length measured is only ~ 9 μm, which is still shorter than the mfp of long wavelength phonons whose contribution to thermal conductivity is not negligible. Actually, for bulk graphite, the length dependence for the thermal conductivity extends to about ~ 10 μm.[170]

For experimental demonstration of superdiffusive transport, it is critical to distinguish the observation from partially ballistic transport. While power law length dependence is a good indication of the superdiffusive behavior, it is important that the lengths of samples span a wide range and go beyond the range where size dependence can also be observed for the corresponding bulk sample, *i.e.*, the length dependence extends well beyond the intrinsic phonon mfp in bulk sample. Moreover, since the intrinsic phonon mfp is a strong function of temperature, partially ballistic transport is expected to demonstrate different trends for the length dependence at different temperatures, while superdiffusive transport would follow a consistent power law length dependence at very different temperatures, as long as the transport is 1D phonon dominant.

The above two criteria are summarized in our recent study of the thermal conductivity of ultra-thin $NbSe_3$ nanowires, which demonstrate a transition from 3D to 1D and length-dependent κ.[98]

However, we did struggle on how to distinguish between superdiffusive transport from partially ballistic transport. What eventually convinced us that we did observe superdiffusive transport of 1D phonons instead of partially ballistic transport is the consistent 1/3 power law length dependence at very different temperatures when 1D phonons dominate the transport process and the deviation from 1/3 power law length dependence at even lower temperature where all 3D phonons are important for the nanowire thermal conductivity (Fig. 7b).[98]

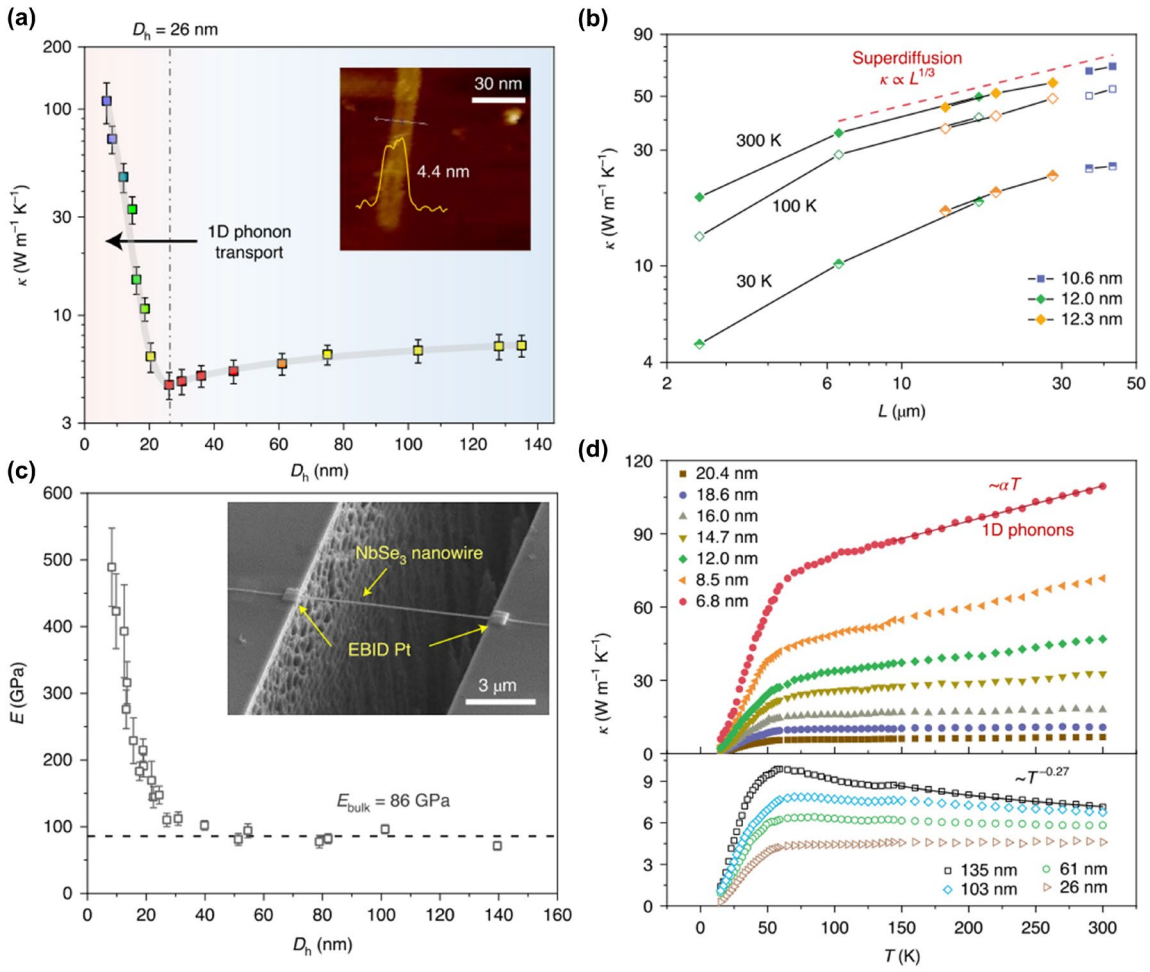

Figure 7. (a) Measured room temperature thermal conductivity κ of $NbSe_3$ nanowires *versus* nanowire hydraulic diameter D_h. The grey solid line is a guide for the eyes. Inset: AFM scanning profile of the nanowire with D_h = 6.8 nm. (b) Measured κ values *versus* suspended length at different temperatures (100 and 300 K) display a 1/3 power-law divergence. The black lines are used to connect the measured thermal conductivity data for the same sample. Note that the deviation from the 1/3 power law at 30 K is because at this temperature, the transport is not 1D phonon dominant. (c) Measured Young's modulus E *versus* D_h, where the average bulk value is plotted as a dashed line. Inset: a SEM image of a $NbSe_3$ nanowire on top of a Si trench with electron-beam-induced deposition (EBID) of Pt at the two edges. (d) Temperature dependence of κ for different diameter wires (the suspended lengths are ~15 μm for all samples). α in the top

panel is a constant. The measured κ for the thickest $NbSe_3$ nanowire (135 nm) demonstrates an $\sim T^{-0.27}$ dependence from 170 to 300 K, signifying the importance of Umklapp scattering. Reproduced with permission from Nat. Nanotechnol. 16, 764 (2021). Copyright Springer Nature Limited 2021.

$NbSe_3$ nanowires belong to a class of quasi-1D van der Waals crystals with covalently bonded atomic chains assembled together *via* weak van der Waals inter-chain interactions. The quasi-1D crystal family includes transition metal chalcogenides (e.g. $NbSe_3$, $TaSe_3$, ZrS_3, $ZrTe_3$, etc.), ternary transition metal chalcogenides (e.g. $Ta_2Pd_3Se_8$, $Ta_2Pt_3Se_8$, Ba_2ZnS_3), as well as other transition metal compounds. In fact, the quasi-1D crystal family is probably as large as 2D materials family but thermal transport properties of this large class of materials are not well explored. Many quasi-1D materials also demonstrate charge-density wave phase-transition with spontaneous condensation of free electrons, which provides unique opportunities for probing the effects of electron-phonon interactions on lattice thermal conductivity.[97,174]

For $NbSe_3$ nanowires, it was recently found that as the nanowire diameter reduces from 135 nm to 26 nm, the thermal conductivity decreases as a result of phonon-boundary scattering; however, as the wire diameter further decreases, the thermal conductivity increases rapidly, with a 25-fold enhancement as the wire diameter reaches 6.8 nm (the lengths of all nanowire samples are ~ 15 μm, Fig. 7a).[98] The trend opposite to the classical size effect for wires of < 26 nm diameter indicates that phonons are likely more and more confined to propagate along the atomic chains with marginal impact from the nanowire surface, which suggests 1D phonon transport. The above analysis was further confirmed by the temperature dependence of the thermal conductivity (Fig. 7d). For larger wires, κ decreases with temperature above 50 K, while for thin wires, κ escalates linearly with temperature, which strongly indicates that additional 1D phonon modes are continuously excited as temperature increases.[98]

Most importantly, examination of the length dependence of κ indicates a transition from a convergent trend for thicker wires to a divergent thermal conductivity for thinner wires and for three wires of 10-12 nm diameter, at both 100 and 300 K, the thermal conductivity demonstrates a consistent 1/3 power law length dependence from ~ 6 μm to 42.5 μm. Note that for thicker wire, κ saturates to a constant value beyond 6 μm. In addition, at even lower temperature of 30 K, where

all 3D phonons are important, the length dependence deviates from the 1/3 power law and tends to saturate for longer samples (Fig. 7b).[98]

Further experimental characterization indicates that the continuous excitation of 1D phonons as temperature increases, which dominate thermal transport at $T > 50$ K for thin wires, is due to greatly enhanced Young's modulus. Here, the Young's modulus of individual $NbSe_3$ nanowires is measured using three-point bending test with AFM. In fact, shown as in Fig. 7c, the Young's modulus starts to increase as the wire diameter becomes smaller than 30 nm and reaches a value of over 5 time the bulk value as the wire diameter reduces to 8.9 nm.[98] The enhanced Young's modulus shifts the Debye temperature to a higher level that allows for additional 1D phonon modes to be excited and alters the phonon dispersion to suppress Umklapp scattering.

One key question in the length dependence study is the contribution of contact thermal resistance with the heat source/sink using the microthermal bridge approach, which could also lead to a length dependent thermal conductivity; and it is critical to distinguish the length dependence as a result of non-Fourier transport from that of contact thermal resistance. The contacts between the nanowire and heat source/sink could have two effects on thermal transport. (1) To pose a contact thermal resistance, R_c, due to the combined effects of restricted contact area, relatively weak van der Waals interactions, and different properties of the materials on each side of the contact. This resistance exists no matter how the nanowire length compares with the phonon mfp, and is constant for the same nanowire even though the sample length between the heat source and sink changes. (2) To confine the phonon mfp if the nanowire length is shorter than the intrinsic phonon mfp in the nanowire. In this case, there will be an additional temperature jump at the contact due to ballistic/superdiffusive phonons. Luckily, the two effects can be distinguished through examining the measured total thermal resistance *versus* sample length.[98] The contact thermal resistance R_c adds a constant to the nanowire resistance and the measured total thermal resistance (R_{tot}) follows a linear trend with length, and the contact thermal resistance can be extracted as the intercept with the vertical axis in the R_{tot} *versus* sample length (L) profile. However, if the contact with the heat source/sink confines the phonon mfp in the nanowire, the R_{tot} *versus* L profile will not be linear. In this case, the thermal conductivity derived from the differential thermal resistance (the resistance difference between two samples of different lengths) will be significantly higher than the effective thermal conductivity derived from the measurement at a specific sample length.

The effect of contact thermal resistance has been a concern often raised in the review process of length dependence of thermal conductivity and hopefully the above discussion clarifies the issue and avoids future confusion in this type of studies.

Summary and outlook

Nanowires provide an ideal platform to explore the lattice thermal conductivity of various technologically important materials as we can effectively tune the phonon boundary scattering strength through adjusting the wire sizes. In addition, different confinement effects allow for both enhancing and reducing the nanowire thermal conductivity, rendering various nanowires themselves as promising materials for engineering applications. For example, super heat conductors can effectively transfer heat from one location to another with minimal heat loss, which can serve as a solid-state heat pipe that can find extensive applications in engineering practice. On the other hand, while nanowires have been projected to be able to enhance the thermoelectric figures of merit as compared to bulk materials, little efforts have been made to integrate different confinement effects, such as the kink morphology and acoustic softening, to reduce the lattice thermal conductivity. In spite of these attractive potential applications, much has to be done before wide deployment of nanowire-based devices. For example, in fabricating nanowire arrays for device level applications, it remains challenging to produce a large amount of nanowires with consistent geometries and high qualities.[175] Also, thermal boundary resistance between the nanostructures and substrate remains an issue for heat dissipation applications.[176] As such, continued progress in nanowire fabrication techniques, and high throughput and high fidelity theoretical predictions are needed to speed up the materials screening and develop high quality and novel nanowire-based devices.

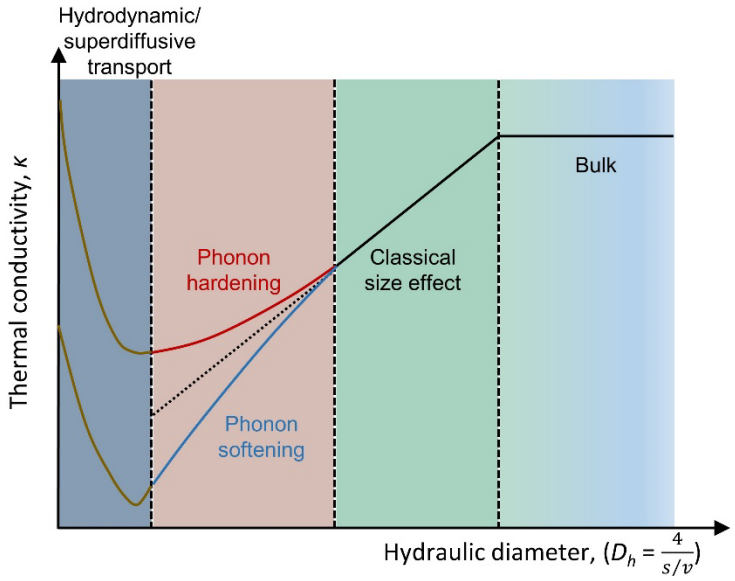

Figure 8. Summary of key factors important for thermal transport in nanowires discussed in this perspective.

For nanowires, owing to the advantage of the additional knob to tune the boundary scattering strength, one can distinguish and dissect the relative contributions of various factors affecting phonon transport. In this perspective, we discussed key factors that are important for thermal transport in nanowires, as shown in a regime map in Fig. 8. In addition, we highlight several promising topics that have yet to be fully explored for furthering the understanding of nanoscale thermal transport through taking the advantage of the unique nanowire system:

(1) While Matthiessen's rule has been widely applied to consider the overall scattering rates of various scattering mechanisms, care has to be used when scattering mechanisms are not independent and implicitly coupled with each other. This can happen when phonon focusing effect becomes important in elastically anisotropic materials;

(2) While the classic size effect is well understood for nanostructures of simple morphologies, it could influence the thermal conductivity in a more subtle manner, as demonstrated in kinked and fishbone nanowires. It is important to study and distinguish the classic size effect in more complex morphology nanostructures from the more intriguing phonon coherence effects, which can lead to exotic heat transport phenomena, such as phonon localizations;

(3) Coupled mechanical/thermal engineering of nanostructures may be a fruitful direction to pursue, which offers a fundamentally new route for structural design/interfacial engineering to construct materials with desirable thermal conductivities, and could also enlighten ideas to dynamically adjust thermal properties on demand through tuning the volumetric strain;

(4) Lastly, there is growing interest to develop thermally conductive materials for heat dissipation to tackle the challenges associated with the high-power density in integrated microelectronics. Here, 1D superdiffusive phonon transport is proposed as a promising mechanism for this purpose. Although experimental observation has confirmed this exotic phenomenon through examining thermal transport in ultra-thin van der Waals crystal nanowires, future research is needed to fully disclose the conditions for superdiffusive phonon transport in van der Waals crystals, which will in turn establish the design principles to leverage this unique mechanism for the development of functional thermal materials and devices.

Acknowledgements: D.L. thanks the financial support from the U.S. National Science Foundation (Award#1805924, 1903645, 2114278).

Conflict of Interest: The authors declare no competing financial interests.

Data Availability: Data sharing is not applicable to this article as no new data were created or analyzed in this study.

References:

[1] M. Fierz and V.F. Weisskopf, *Theoretical Physics in the Twentieth Century: A Memorial Volume to Wolfgang Pauli* (Wiley, New York, 1951).

[2] R. Chen, J. Lee, W. Lee, and D. Li, Chem. Rev. **119**, 9260 (2019).

[3] Bozhi Tian, T. J. Kempa, and C. M. Lieber, Chem. Soc. Rev. **38**, 16 (2008).

[4] J. Deng, Y. Su, D. Liu, P. Yang, B. Liu, and C. Liu, Chem. Rev. **119**, 9221 (2019).

[5] X. Qian, J. Zhou, and G. Chen, Nat. Mater. 1 (2021).

[6] Y. Li, W. Li, T. Han, X. Zheng, J. Li, B. Li, S. Fan, and C.W. Qiu, Nat. Rev. Mater. (2021).

[7] L. Yang, M.P. Gordon, A.K. Menon, A. Bruefach, K. Haas, M.C. Scott, R.S. Prasher, and J.J.

Urban, Sci. Adv. **7**, eabe6000 (2021).

[8] F. Patolsky, G. Zheng, and C.M. Lieber, Nanomedicine **1**, 51 (2006).

[9] P. Ambhorkar, Z. Wang, H. Ko, S. Lee, K. Koo, K. Kim, and D. (Dan) Cho, Micromachines **9**, (2018).

[10] C.M. Lieber and Z.L. Wang, MRS Bull. **32**, 99 (2007).

[11] L.D. Hicks and M.S. Dresselhaus, Phys. Rev. B **47**, 16631 (1993).

[12] L.D. Hicks and M.S. Dresselhaus, Phys. Rev. B **47**, 12727 (1993).

[13] J. Heremans and C.M. Thrush, Phys. Rev. B **59**, 12579 (1999).

[14] M.S. Dresselhaus, G. Dresselhaus, X. Sun, Z. Zhang, S.B. Cronin, T. Koga, J.Y. Ying, and G. Chen, Microscale Thermophys. Eng. **3**, 89 (1999).

[15] M.S. Dresselhaus, Y.M. Lin, G. Dresselhaus, X. Sun, Z. Zhang, S.B. Cronin, T. Koga, and J.Y. Ying, Int. Conf. Thermoelectr. ICT, Proc. 92 (1999).

[16] S. Shen, A. Henry, J. Tong, R. Zheng, and G. Chen, Nat. Nanotechnol. **5**, 251 (2010).

[17] D. Li, Y. Wu, P. Kim, L. Shi, P. Yang, and A. Majumdar, Appl. Phys. Lett. **83**, 2934 (2003).

[18] S. Sett, V.K. Aggarwal, A. Singha, and A.K. Raychaudhuri, Phys. Rev. Appl. **13**, 054008 (2020).

[19] J.W. Roh, K. Hippalgaonkar, J.H. Ham, R. Chen, M.Z. Li, P. Ercius, A. Majumdar, W. Kim, and W. Lee, ACS Nano **5**, 3954 (2011).

[20] C.T. Bui, R. Xie, M. Zheng, Q. Zhang, C.H. Sow, B. Li, and J.T.L. Thong, Small **8**, 738 (2012).

[21] C. Guthy, C.Y. Nam, and J.E. Fischer, J. Appl. Phys. **103**, 064319 (2008).

[22] M.M. Rojo, S. Grauby, J.-M. Rampnoux, O. Caballero-Calero, M. Martin-Gonzalez, and S. Dilhaire, J. Appl. Phys. **113**, 054308 (2013).

[23] M. Soini, I. Zardo, E. Uccelli, S. Funk, G. Koblmüller, A. Fontcuberta i Morral, and G. Abstreiter, Appl. Phys. Lett. **97**, 263107 (2010).

[24] D. Vakulov, S. Gireesan, M.Y. Swinkels, R. Chavez, T. Vogelaar, P. Torres, A. Campo, M. De

Luca, M.A. Verheijen, S. Koelling, L. Gagliano, J.E.M. Haverkort, F.X. Alvarez, P.A. Bobbert, I. Zardo, and E.P.A.M. Bakkers, Nano Lett. **20**, 2703 (2020).

[25] N. Mingo, L. Yang, D. Li, and A. Majumdar, Nano Lett. **3**, 1713 (2003).

[26] Q. Zhang, Z. Cui, Z. Wei, S.Y. Chang, L. Yang, Y. Zhao, Y. Yang, Z. Guan, Y. Jiang, J. Fowlkes, J. Yang, D. Xu, Y. Chen, T.T. Xu, and D. Li, Nano Lett. **17**, 3550 (2017).

[27] L. Yang, Q. Zhang, Z. Wei, Z. Cui, Y. Zhao, T.T. Xu, J. Yang, and D. Li, J. Appl. Phys. **126**, 2 (2019).

[28] Y. Zhao, L. Yang, C. Liu, Q. Zhang, Y. Chen, J. Yang, and D. Li, Int. J. Heat Mass Transf. **137**, (2019).

[29] L. Yang, Y. Zhao, Q. Zhang, J. Yang, and D. Li, Nanoscale **11**, 8196 (2019).

[30] J. Maire, R. Anufriev, T. Hori, J. Shiomi, S. Volz, and M. Nomura, Sci. Rep. **8**, 4452 (2018).

[31] W. Park, G. Romano, E.C. Ahn, T. Kodama, J. Park, M.T. Barako, J. Sohn, S.J. Kim, J. Cho, A.M. Marconnet, M. Asheghi, A.M. Kolpak, and K.E. Goodson, Sci. Rep. **7**, 6233 (2017).

[32] Y. Xiao, D. Xu, F.J. Medina, S. Wang, and Q. Hao, Mater. Today Phys. **12**, 100179 (2020).

[33] A.I. Hochbaum, R. Chen, R.D. Delgado, W. Liang, E.C. Garnett, M. Najarian, A. Majumdar, and P. Yang, Nature **451**, 163 (2008).

[34] J. Lim, K. Hippalgaonkar, S.C. Andrews, and A. Majumdar, Nano Lett. **12**, 2475 (2012).

[35] Y. Zhu, F. Xu, Q. Qin, W.Y. Fung, and W. Lu, Nano Lett. **9**, 3934 (2009).

[36] M.C. Wingert, S. Kwon, M. Hu, D. Poulikakos, J. Xiang, and R. Chen, Nano Lett. **15**, 2605 (2015).

[37] L. Yang, Y. Yang, Q. Zhang, Y. Zhang, Y. Jiang, Z. Guan, M. Gerboth, J. Yang, Y. Chen, D. Greg Walker, T.T. Xu, and D. Li, Nanoscale **8**, 17895 (2016).

[38] T.H. Chang, G. Cheng, C. Li, and Y. Zhu, Extrem. Mech. Lett. **8**, 177 (2016).

[39] J.H. Yoo, S.I. Oh, and M.S. Jeong, J. Appl. Phys. **107**, 094316 (2010).

[40] J.Y. Wu, S. Nagao, J.Y. He, and Z.L. Zhang, Nano Lett. **11**, 5264 (2011).

[41] S. Cuenot, C. Frétigny, S. Demoustier-Champagne, and B. Nysten, Phys. Rev. B **69**, 165410

(2004).

[42] R.A. Bernal, R. Agrawal, B. Peng, K.A. Bertness, N.A. Sanford, A. V. Davydov, and H.D. Espinosa, Nano Lett. **11**, 548 (2011).

[43] C.Q. Chen, Y. Shi, Y.S. Zhang, J. Zhu, and Y.J. Yan, Phys. Rev. Lett. **96**, 075505 (2006).

[44] J. Boh, *Thermal Transport in Low Dimensions: From Statistical Physics to Nanoscale Heat Transfer* (Springer Nature, 2016).

[45] K. Fuchs, Math. Proc. Cambridge Philos. Soc. **34**, 100 (1938).

[46] E.H. Sondheimer, Adv. Phys. **1**, 1 (1952).

[47] D. Kojda, R. Mitdank, M. Handwerg, A. Mogilatenko, M. Albrecht, Z. Wang, J. Ruhhammer, M. Kroener, P. Woias, and S.F. Fischer, Phys. Rev. B **91**, 024302 (2015).

[48] Y. Tao, Y. Zhao, M. Akter, T.T. Xu, Y. Chen, and D. Li, Appl. Phys. Lett. **118**, 153105 (2021).

[49] K. Fuchs, Math. Proc. Cambridge Philos. Soc. **34**, 100 (1938).

[50] G. De Marzi, D. Iacopino, A.J. Quinn, and G. Redmond, J. Appl. Phys. **96**, 3458 (2004).

[51] W. Ma, X. Zhang, and K. Takahashi, J. Phys. D. Appl. Phys. **43**, 465301 (2010).

[52] Y. Zhao, M.L. Fitzgerald, Y. Tao, Z. Pan, G. Sauti, D. Xu, Y.Q. Xu, and D. Li, Nano Lett. **20**, 7389 (2020).

[53] J. Ziman, *Electrons and Phonons: The Theory of Transport Phenomena in Solids* (Oxford University Press (OUP), 2001).

[54] D. Josell, S.H. Brongersma, and Z. Tőkei, Annu. Rev. Mater. Res. **39**, 231 (2009).

[55] R.G. Chambers, Proc. R. Soc. A Math. Phys. Eng. Sci. **202**, 378 (1950).

[56] W. Park, D.D. Shin, S.J. Kim, J.S. Katz, J. Park, C.H. Ahn, T. Kodama, M. Asheghi, T.W. Kenny, and K.E. Goodson, Appl. Phys. Lett. **110**, 213102 (2017).

[57] W. Zhang, S.H. Brongersma, Z. Li, D. Li, O. Richard, and K. Maex, J. Appl. Phys. **101**, 063703 (2007).

[58] S. Kim, H. Suhl, and I.K. Schuller, Phys. Rev. Lett. **78**, 322 (1997).

[59] Y.P. Timalsina, A. Horning, R.F. Spivey, K.M. Lewis, T.-S. Kuan, G.-C. Wang, and T.-M. Lu, Nanotechnology **26**, 075704 (2015).

[60] A. Bid, A. Bora, and A.K. Raychaudhuri, Phys. Rev. B **74**, 035426 (2006).

[61] W. Zhang, S.H. Brongersma, Z. Li, D. Li, O. Richard, and K. Maex, J. Appl. Phys. **101**, 063703 (2007).

[62] G. De Marzi, D. Iacopino, A.J. Quinn, and G. Redmond, J. Appl. Phys. **96**, 3458 (2004).

[63] M.V. Kamalakar and A.K. Raychaudhuri, New J. Phys. **14**, 043032 (2012).

[64] A. Bid, A. Bora, and A.K. Raychaudhuri, Phys. Rev. B **74**, 035426 (2006).

[65] M.V. Kamalakar and A.K. Raychaudhuri, New J. Phys. **14**, 043032 (2012).

[66] Y.P. Timalsina, A. Horning, R.F. Spivey, K.M. Lewis, T.-S. Kuan, G.-C. Wang, and T.-M. Lu, Nanotechnology **26**, 075704 (2015).

[67] C. Adelmann, Solid. State. Electron. **152**, 72 (2019).

[68] W. Ma, X. Zhang, and K. Takahashi, J. Phys. D. Appl. Phys. **43**, 465301 (2010).

[69] S. Kim, H. Suhl, and I.K. Schuller, Phys. Rev. Lett. **78**, 322 (1997).

[70] T.H. Chang, G. Cheng, C. Li, and Y. Zhu, Extrem. Mech. Lett. **8**, 177 (2016).

[71] J.H. Yoo, S.I. Oh, and M.S. Jeong, J. Appl. Phys. **107**, 094316 (2010).

[72] J.Y. Wu, S. Nagao, J.Y. He, and Z.L. Zhang, Nano Lett. **11**, 5264 (2011).

[73] D.G. Cahill, W.K. Ford, K.E. Goodson, G.D. Mahan, A. Majumdar, H.J. Maris, R. Merlin, and S.R. Phillpot, J. Appl. Phys. **93**, 793 (2003).

[74] D.G. Cahill, P. V. Braun, G. Chen, D.R. Clarke, S. Fan, K.E. Goodson, P. Keblinski, W.P. King, G.D. Mahan, A. Majumdar, H.J. Maris, S.R. Phillpot, E. Pop, and L. Shi, Appl. Phys. Rev. **1**, 011305 (2014).

[75] Y.S. Ju and K.E. Goodson, Appl. Phys. Lett. **74**, 3005 (1999).

[76] K. Esfarjani, G. Chen, and H.T. Stokes, Phys. Rev. B - Condens. Matter Mater. Phys. **84**, 085204 (2011).

[77] K.T. Regner, D.P. Sellan, Z. Su, C.H. Amon, A.J.H. McGaughey, and J. Malen, Nat.

Commun. **4**, 1640 (2013).

[78] J. Yang, M. Shen, Y. Yang, W.J. Evans, Z. Wei, W. Chen, A. a. Zinn, Y. Chen, R. Prasher, T.T. Xu, P. Keblinski, and D. Li, Phys. Rev. Lett. **112**, 1 (2014).

[79] Q. Fu, J. Yang, Y. Chen, D. Li, and D. Xu, Appl. Phys. Lett. **106**, 031905 (2015).

[80] Z. Wei, J. Yang, W. Chen, K. Bi, D. Li, and Y. Chen, Appl. Phys. Lett. **104**, 081903 (2014).

[81] H. Zhang, X. Chen, Y.D. Jho, and A.J. Minnich, Nano Lett. **16**, 1643 (2016).

[82] Z. Pan, Y. Tao, Y. Zhao, M.L. Fitzgerald, J.R. McBride, L. Zhu, and D. Li, Nano Lett. **21**, 7317 (2021).

[83] Y. Hu, L. Zeng, A.J. Minnich, M.S. Dresselhaus, and G. Chen, Nat. Nanotechnol. **10**, 701 (2015).

[84] M.E. Siemens, Q. Li, R. Yang, K.A. Nelson, E.H. Anderson, M.M. Murnane, and H.C. Kapteyn, Nat. Mater. **9**, 26 (2009).

[85] K.M. Hoogeboom-Pot, J.N. Hernandez-Charpak, X. Gu, T.D. Frazer, E.H. Anderson, W. Chao, R.W. Falcone, R. Yang, M.M. Murnane, H.C. Kapteyn, and D. Nardi, Proc. Natl. Acad. Sci. U. S. A. **112**, 4846 (2015).

[86] L. Shi, D. Li, C. Yu, W. Jang, D. Kim, Z. Yao, P. Kim, and A. Majumdar, J. Heat Transfer **125**, 881 (2003).

[87] P. Kim, L. Shi, a Majumdar, and P.L. McEuen, Phys. Rev. Lett. **87**, 215502 (2001).

[88] A.L. Moore and L. Shi, Meas. Sci. Technol. **22**, 015103 (2010).

[89] M.C. Wingert, Z.C.Y. Chen, S. Kwon, J. Xiang, and R. Chen, Rev. Sci. Instrum. **83**, 024901 (2012).

[90] A. Weathers and L. Shi, Annu. Rev. Heat Transf. **16**, 101 (2013).

[91] J. Callaway, Phys. Rev. **113**, 1046 (1959).

[92] M. Holland, Phys. Rev. **132**, 2461 (1963).

[93] M.G. Holland, Phys. Rev. **134**, A471 (1964).

[94] M. Asen-Palmer, K. Bartkowski, E. Gmelin, M. Cardona, A. Zhernov, A. Inyushkin, A.

Taldenkov, V. Ozhogin, K. Itoh, and E. Haller, Phys. Rev. B **56**, 9431 (1997).

[95] N. Mingo, Phys. Rev. B **68**, 113308 (2003).

[96] Q. Zhang, C. Liu, X. Liu, J. Liu, Z. Cui, Y. Zhang, L. Yang, Y. Zhao, T.T. Xu, Y. Chen, J. Wei, Z. Mao, and D. Li, ACS Nano **12**, 2634 (2018).

[97] L. Yang, Y. Tao, J. Liu, C. Liu, Q. Zhang, M. Akter, Y. Zhao, T.T. Xu, Y. Xu, Z. Mao, Y. Chen, and D. Li, Nano Lett. **19**, 415 (2019).

[98] L. Yang, Y. Tao, Y. Zhu, M. Akter, K. Wang, Z. Pan, Y. Zhao, Q. Zhang, Y.Q. Xu, R. Chen, T.T. Xu, Y. Chen, Z. Mao, and D. Li, Nat. Nanotechnol. **16**, 764 (2021).

[99] L. Yang, D. Huh, R. Ning, V. Rapp, Y. Zeng, Y. Liu, S. Ju, Y. Tao, Y. Jiang, J. Beak, J. Leem, S. Kaur, H. Lee, X. Zheng, and R.S. Prasher, Nat. Commun. 2021 121 **12**, 1 (2021).

[100] Z. Wang and N. Mingo, Appl. Phys. Lett. **97**, 101903 (2010).

[101] F. Zhou, A.L. Moore, J. Bolinsson, A. Persson, L. Fröberg, M.T. Pettes, H. Kong, L. Rabenberg, P. Caroff, D.A. Stewart, N. Mingo, K.A. Dick, L. Samuelson, H. Linke, and L. Shi, Phys. Rev. B - Condens. Matter Mater. Phys. **83**, 1 (2011).

[102] J.W. Roh, S.Y. Jang, J. Kang, S. Lee, J.-S. Noh, W. Kim, J. Park, and W. Lee, Appl. Phys. Lett. **96**, 103101 (2010).

[103] J. Yang, H. Tang, Y. Zhao, Y. Zhang, J. Li, Z. Ni, Y. Chen, and D. Xu, Nanoscale **7**, 16071 (2015).

[104] M. Nomura and J. Maire, J. Electron. Mater. **44**, 1426 (2015).

[105] J.W. Jiang, N. Yang, B.S. Wang, and T. Rabczuk, Nano Lett. **13**, 1670 (2013).

[106] J.-K. Yu, S. Mitrovic, D. Tham, J. Varghese, and J.R. Heath, Nat. Nanotechnol. **5**, 718 (2010).

[107] N. Zen, T.A. Puurtinen, T.J. Isotalo, S. Chaudhuri, and I.J. Maasilta, Nat. Commun. **5**, 3435 (2014).

[108] J. Lee, W. Lee, G. Wehmeyer, S. Dhuey, D.L. Olynick, S. Cabrini, C. Dames, J.J. Urban, and P. Yang, Nat. Commun. **8**, 14054 (2017).

[109] A. Jain, Y.J. Yu, and A.J.H. McGaughey, Phys. Rev. B - Condens. Matter Mater. Phys. **87**,

195301 (2013).

[110] J. Ravichandran, A.K. Yadav, R. Cheaito, P.B. Rossen, A. Soukiassian, S.J. Suresha, J.C. Duda, B.M. Foley, C.-H. Lee, Y. Zhu, A.W. Lichtenberger, J.E. Moore, D.A. Muller, D.G. Schlom, P.E. Hopkins, A. Majumdar, R. Ramesh, and M.A. Zurbuchen, Nat. Mater. **13**, 168 (2013).

[111] M.N. Luckyanova, J. Garg, K. Esfarjani, A. Jandl, M.T. Bulsara, A.J. Schmidt, A.J. Minnich, S. Chen, M.S. Dresselhaus, Z. Ren, E.A. Fitzgerald, and G. Chen, Science (80-.). **338**, 936 (2012).

[112] D. Ding, X. Yin, and B. Li, New J. Phys. **20**, 023008 (2018).

[113] E. Henriksen, K. Schwab, J. Worlock, and M. Roukes, Nature **404**, 974 (2000).

[114] P.J. Koppinen and I.J. Maasilta, Phys. Rev. Lett. **102**, 165502 (2009).

[115] A. Tavakoli, K. Lulla, T. Crozes, N. Mingo, E. Collin, and O. Bourgeois, Nat. Commun. **9**, 4287 (2018).

[116] G.A. Slack, Solid State Phys. - Adv. Res. Appl. **34**, 1 (1979).

[117] Y. Chen, D. Li, J.R. Lukes, and A. Majumdar, J. Heat Transfer **127**, 1129 (2005).

[118] D. Lacroix, K. Joulain, D. Terris, and D. Lemonnier, Appl. Phys. Lett. **89**, 103104 (2006).

[119] P. Chantrenne, J.L. Barrat, X. Blase, and J.D. Gale, J. Appl. Phys. **97**, 104318 (2005).

[120] A.J.H. McGaughey, E.S. Landry, D.P. Sellan, and C.H. Amon, Appl. Phys. Lett. **99**, 20 (2011).

[121] M.C. Wingert, Z.C.Y. Chen, E. Dechaumphai, J. Moon, J.H. Kim, J. Xiang, and R. Chen, Nano Lett. **11**, 5507 (2011).

[122] L.M. Bellan, J. Kameoka, and H.G. Craighead, Nanotechnology **16**, 1095 (2005).

[123] Y. Calahorra, O. Shtempluck, V. Kotchetkov, and Y.E. Yaish, Nano Lett. **15**, 2945 (2015).

[124] H. Ni and X. Li, Nanotechnology **17**, 3591 (2006).

[125] Y. Zhang, X. Zhang, L. Yang, Q. Zhang, M.L. Fitzgerald, A. Ueda, Y. Chen, R. Mu, D. Li, and L.M. Bellan, Soft Matter **14**, 9534 (2018).

[126] W. Liu and M. Asheghi, J. Heat Transfer **128**, 75 (2006).

[127] Y. Li, F. Qian, J. Xiang, and C.M. Lieber, Mater. Today **9**, 18 (2006).

[128] F. Qian, Y. Li, S. Gradečak, D. Wang, C.J. Barrelet, and C.M. Lieber, Nano Lett. **4**, 1975 (2004).

[129] B. Tian, X. Zheng, T.J. Kempa, Y. Fang, N. Yu, G. Yu, J. Huang, and C.M. Lieber, Nature **449**, 885 (2007).

[130] G. Zhang, W. Wang, and X. Li, Adv. Mater. **20**, 3654 (2008).

[131] E.P. Pokatilov, D.L. Nika, and A.A. Balandin, Phys. Rev. B - Condens. Matter Mater. Phys. **72**, 113311 (2005).

[132] M. Hu, K.P. Giapis, J. V. Goicochea, X. Zhang, and D. Poulikakos, Nano Lett. **11**, 618 (2011).

[133] J. Chen, G. Zhang, and B. Li, J. Chem. Phys. **135**, 104508 (2011).

[134] J. Kang, J.W. Roh, W. Shim, J. Ham, J.-S. Noh, and W. Lee, Adv. Mater. **23**, 3414 (2011).

[135] S. Ning, S.C. Huberman, Z. Ding, H.H. Nahm, Y.H. Kim, H.S. Kim, G. Chen, and C.A. Ross, Adv. Mater. **31**, (2019).

[136] A. Sarantopoulos, W.-L. Ong, J.A. Malen, and F. Rivadulla, Appl. Phys. Lett. **113**, 182902 (2018).

[137] M.W. Bockrath, D.H. Cobden, J. Lu, A.G. Rinzler, R.E. Smalley, L. Balents, and P.L. McEuen, Nature **397**, 598 (1999).

[138] L. Cui, S. Hur, Z.A. Akbar, J.C. Klöckner, W. Jeong, F. Pauly, S.Y. Jang, P. Reddy, and E. Meyhofer, Nature **572**, 628 (2019).

[139] L. Cui, W. Jeong, S. Hur, M. Matt, J.C. Klöckner, F. Pauly, P. Nielaba, J.C. Cuevas, E. Meyhofer, and P. Reddy, Science (80-.). **355**, 1192 (2017).

[140] T. Meier, F. Menges, P. Nirmalraj, H. Hölscher, H. Riel, and B. Gotsmann, Phys. Rev. Lett. **113**, 060801 (2014).

[141] R. Livi and S. Lepri, Nature **421**, 327 (2003).

[142] E. Fermi, P. Pasta, S. Ulam, and M. Tsingou., No. LA-1940. Los Alamos Sci. Lab. (1955).

[143] S. Lepri, R. Livi, and A. Politi, Phys. Rev. Lett. **78**, 1896 (1997).

[144] S. Lepri, Eur. Phys. J. B **18**, 441 (2000).

[145] S. Liu, X.F. Xu, R.G. Xie, G. Zhang, and B.W. Li, Eur. Phys. J. B **85**, 337 (2012).

[146] Z. Zhang, Y. Ouyang, Y. Cheng, J. Chen, N. Li, and G. Zhang, Phys. Rep. **860**, 1 (2020).

[147].

[148] R. Livi, M. Pettini, S. Ruffo, M. Sparpaglione, and A. Vulpiani, Phys. Rev. A **31**, 1039 (1985).

[149] M. Toda, Phys. Rep. **18**, 1 (1975).

[150] N.J. Zabusky, Comput. Phys. Commun. **5**, 1 (1973).

[151] M. Toda, Phys. Scr. **20**, 424 (1979).

[152] J. Ford, Phys. Rep. **213**, 271 (1992).

[153] G. Casati, J. Ford, F. Vivaldi, and W.M. Visscher, Phys. Rev. Lett. **52**, 1861 (1984).

[154] N. Li, B. Li, and S. Flach, Phys. Rev. Lett. **105**, 054102 (2010).

[155] S. Lepri, R. Livi, and A. Politi, Europhys. Lett. **43**, 271 (1998).

[156] O. Narayan and S. Ramaswamy, Phys. Rev. Lett. **89**, 200601 (2002).

[157] S. Lepri, R. Livi, and A. Politi, Phys. Rev. E **68**, 8 (2003).

[158] J.S. Wang and B. Li, Phys. Rev. Lett. **92**, 074302 (2004).

[159] J.S. Wang and B. Li, Phys. Rev. E **70**, 16 (2004).

[160] Z. Zhang, Y. Ouyang, Y. Cheng, J. Chen, N. Li, and G. Zhang, Phys. Rep. **860**, 1 (2020).

[161] O. Narayan and S. Ramaswamy, Phys. Rev. Lett. **89**, 200601 (2002).

[162] A. Pereverzev, Phys. Rev. E **68**, 056124 (2003).

[163] A. Henry and G. Chen, Phys. Rev. Lett. **101**, 235502 (2008).

[164] A. Henry, G. Chen, S.J. Plimpton, and A. Thompson, Phys. Rev. B **82**, 144308 (2010).

[165] Y. Zhou, X. Zhang, and M. Hu, Nano Lett. **17**, 1269 (2017).

[166] N. Yang, G. Zhang, and B. Li, Nano Today **5**, 85 (2010).

[167] X. Xu, L.F.C. Pereira, Y. Wang, J. Wu, K. Zhang, X. Zhao, S. Bae, C. Tinh Bui, R. Xie, J.T.L. Thong, B.H. Hong, K.P. Loh, D. Donadio, B. Li, and B. Özyilmaz, Nat. Commun. **5**, 3689 (2014).

[168] C.W. Chang, D. Okawa, H. Garcia, A. Majumdar, and A. Zettl, Phys. Rev. Lett. **101**, 1 (2008).

[169] V. Lee, C.H. Wu, Z.X. Lou, W.L. Lee, and C.W. Chang, Phys. Rev. Lett. **118**, 135901 (2017).

[170] G. Fugallo, A. Cepellotti, L. Paulatto, M. Lazzeri, N. Marzari, and F. Mauri, Nano Lett. **14**, 6109 (2014).

[171] Q.-Y. Li, K. Takahashi, and X. Zhang, Phys. Rev. Lett. **119**, 179601 (2017).

[172] Q.Y. Li, ArXiv (2017).

[173] V. Lee, C.H. Wu, Z.X. Lou, W.L. Lee, and C.W. Chang, ArXiv (2018).

[174] Z. Pan, L. Yang, Y. Tao, Y. Zhu, Y.Q. Xu, Z. Mao, and D. Li, Phys. Chem. Chem. Phys. **22**, 21131 (2020).

[175] D. Rawtani, T. Sajan, A. Twinkle, and Y.K. Agrawal, Adv. Mater. Sci **40**, 177 (2015).

[176] A.L. Moore and L. Shi, Mater. Today **17**, 163 (2014).